University of Stavanger

Faculty of Science and Technology

MASTER'S THESIS

Study program/Specialization: Engineering Structures and Materials – Civil engineering structures	Spring semester, 2024 Open or ~~Confidential~~
Writer: Maoulana-Hamza Yacoub	
Faculty supervisor: Professor Mudiyan Nirosha Damayanthi Adasooriya	
Thesis title: Fatigue life assessment of steel bridges: Interaction effect of Environment- Assisted Cracking and traffic loads	
Credits (ECTS): 30	
Key words: Steel bridge, Railway bridge Riveted, Corrosion fatigue, Damage accumulation, Fatigue life, S-N curve,	Number of pages: 78 + appendix: 13 Stavanger 15. June 2024

Front page of the master's thesis

Faculty of Science and Technology

Fatigue life assessment of steel bridges: Interaction effect of Environment - Assisted Cracking and traffic loads

by

Maoulana-Hamza Yacoub

Department of Mechanical and Structural Engineering and Materials
Science Faculty of Science and Technology
2024

Keywords Steel bridge, Railway bridges, Riveted, Corrosion fatigue, Damage accumulation, S-N curve, Fatigue life,

Abstract

The purpose of this thesis is to investigate the fatigue life of a steel railway bridge in Norway.

Fatigue life is usually determined by conventional approaches such as the λ-coefficient method or the Miner's damage accumulation method.

These methods are pertinent for most of the bridge cases, however they were design for current bridges. Many of the bridges in use nowadays were built at the beginning of the 20^{th} century. These bridges are maintained in life because they are cheaper to keep and maintain them than constructing new bridges. These bridge experience an increase in traffic loads and are exposed to continuous environmental deterioration due to corrosion. This lead to a phenomenon known as corrosion fatigue (CF).

These old bridges, therefore, necessitate new approaches for fatigue life assessment, adapted to their characteristics and current conditions. New fatigue curves (S-N curves) has been developed by Adassoriya et al. for riveted details exposed to a corrosive environment, and adapted to railway bridges.

This method is applied to some members of the bridge, and the results are compared to the Miner's damage rule. A total of 10 members are studied.

The results has revealed a reduction of fatigue live in the range of 12-83 %. The main observed factors that influenced the percentage loss of fatigue life are: the cross-sectional parameters (i.e cross-sectional area, second moment of area), the type of cross-sections, the locations of the members, and the applied traffic load (traffic mix).

To simplify the analysis, some assumptions were made, such as the bridge design and members remaining unchanged from 1906.

The new method developed by Adassoriya et al. [1] propose an innovative approach for the fatigue life assessment of old bridge exposed to corrosion fatigue.

Preface

This report was written as part of my Master's thesis in Structural Engineering at the University of Stavanger, Norway. This project was assigned and supervised by Professor Nirosha D. Adasooriya and falls within the field of fatigue life assessment of metallic structures. Specifically, it aims to evaluate the fatigue life of a railway bridge subjected to repetitive loads in a corrosive environment, a phenomenon also known as fatigue-corrosion.

Firstly, I would like to thank my professor and supervisor, Nirosha D. Adasooriya, for her continuous support throughout this research and writing period. She has been attentive to my inquiries and provided the necessary guidance to successfully conduct this study.

I would like to extend my thanks to Skar Tormod Barland, our associate from Bane Nor, for providing us with the necessary information about the investigated bridge. The name of the bridge is " Bru over Tødola," meaning "brigde above the river Todøla" in english, and was built in 1906.

Finally, I would like to thank my family and friends for their support and for reviewing my work and providing constructive feedback.
Their advice has been crucial, demonstrating the value of considering different perspectives.

This project took place in the spring of 2024 and was submitted in June 2024, in Norway.

Contents

Abstract i

Preface ii

1 Introduction 1
- 1.1 Background and Motivation . . . 1
- 1.2 Aim and objectives . . . 1
- 1.3 Significance . . . 2
- 1.4 Scope and limitations . . . 2
- 1.5 Outline: Thesis structure . . . 3

2 Literature review 5
- 2.1 Fatigue . . . 5
  - 2.1.1 History of fatigue . . . 5
  - 2.1.2 Case histories of bridges failed due to fatigue . . . 6
  - 2.1.3 Fatigue mechanism . . . 6
  - 2.1.4 Methods for fatigue life evaluations . . . 7
  - 2.1.5 Fatigue stresses . . . 8
- 2.2 Corrosion . . . 9
  - 2.2.1 Electrochemical process of corrosion . . . 9
  - 2.2.2 Corrosion mechanism of an iron F_e . . . 11
  - 2.2.3 Types of corrosion . . . 12
  - 2.2.4 Effects of corrosion on steel bridges . . . 13
  - 2.2.5 Factors influencing the rate and progression of corrosion . . . 14
  - 2.2.6 Corrosion prevention . . . 15
  - 2.2.7 Importance of corrosion . . . 16
  - 2.2.8 Case histories of bridge failures due to corrosion . . . 16
- 2.3 Environment-Assisted Cracking . . . 17
  - 2.3.1 Corrosion Fatigue (CF) . . . 18
  - 2.3.2 Stress Corrosion Cracking (SCC) . . . 19
  - 2.3.3 Hydrogen Embrittlement (HE) . . . 20
- 2.4 Structural metals for bridges . . . 20
  - 2.4.1 Cast iron . . . 20
  - 2.4.2 Puddled iron (or Wrought iron) . . . 21
  - 2.4.3 Mild steel (steel) . . . 21
- 2.5 Mechanical properties of century-old railway bridges . . . 21
  - 2.5.1 Experimental study on an old bridge in Norway . . . 21
  - 2.5.2 Recommended values from standards and local guidelines . . . 24
  - 2.5.3 Comparison of material properties . . . 25
- 2.6 Riveted connections in bridges . . . 26

3 Methodology 27
- 3.1 European standards for bridge design and fatigue life assessment . . . 27
  - 3.1.1 EN 1990: Basis of structural design . . . 27
  - 3.1.2 EN 1991-2: Actions on structures - Traffic loads on bridges . . . 28
  - 3.1.3 EN 1993-2: Design of steel structures - Steel Bridges . . . 28
  - 3.1.4 EN 1993-1-9: Design of steel structures – Fatigue . . . 28
- 3.2 Fatigue design with the Palmgren-Miner damage accumulation method . . . 32
- 3.3 Fatigue Load Models for the cumulative damage method . . . 33
  - 3.3.1 Standard traffic mix . . . 35

3.3.2 Light traffic mix . . . 35
3.3.3 Heavy traffic mix . . . 35
3.4 Methodology used for modeling and structural analysis . . . 36

4 Fatigue assessment of bridges in corrosive environment 38
4.1 Proposed fatigue strength for riveted details in corrosive environment . . . 38
4.2 Determination of corrosion wastage and effective cross-sectional parameters for corroded members . . . 40
4.2.1 Corrosion wastage . . . 41
4.2.2 Effective cross-sectional parameters: $A_{\text{eff}}(t)$ and $I_{\text{eff}}(t)$ . . . 42
4.3 Determining the fatigue life of corroded members . . . 43

5 Assessment guidelines for fatigue life of existing steel bridges 45

6 Case study 47
6.1 General description of the bridge . . . 47
6.2 Design material properties . . . 48
6.3 Simplifications, Assumptions . . . 48
6.4 Cross-sections of the bridge . . . 49
6.5 Geometry and modeling in SAP2000 . . . 51
6.6 Corrosion on the bridge . . . 52

7 Results 56
7.1 Critical fatigue life, without corrosion . . . 56
7.2 Reduced fatigue life considering corrosion . . . 56

8 Discussion 59
8.1 Extreme fatigue life without considering corrosion . . . 59
8.1.1 Cross-girder members (CG-edge) . . . 59
8.2 Reduced fatigue life due to corrosion . . . 60
8.2.1 Individual observations . . . 60
8.2.2 Global observations . . . 61
8.3 Differences between the two methods for fatigue life assessment . . . 61
8.4 Reliability of the results and reflection on the results . . . 61

9 Conclusion 62
9.1 Conclusion and Summary . . . 62
9.2 Further work . . . 64

A Appendix: Bridge drawing I

B Appendix: Additional illustrations of the bridge modeling II

C Appendix: Fatigue life inferior to 50 years, of members of the bridge IV

D Appendix: Cross-sections of the bridge VI

E Appendix: Train types used for railway bridges fatigue assessment [EN 1991-2] XIII

List of Figures

2.1 Fatigue progress and failure of a bolt [12] . . . 7
2.2 Simplified corrosion process: a basic wet corrosion cell [15] . . . 10
2.3 The main forms of corrosion [20] . . . 12
2.4 Condensed list of the galvanic series for most common metals [15] . . . 13
2.5 Main conditions for EAC to occur [24] . . . 17
2.6 S-N curve for steels subjected to cyclic stress [14] . . . 18
2.7 Corrosion-fatigue crack in mild steel sheet (250x) [14] . . . 19
2.8 Results of the tensile tests of all specimens [25] . . . 22
2.9 Beam from the bridge and the sample measurements for tensile tests [25] . . . 23
3.1 Standards and guidelines used for fatigue assessment in this paper . . . 27
3.2 Fatigue strength curves for direct stress ranges [31] . . . 29
3.3 Fatigue strength curve with the reference stress ranges . . . 31
3.4 Fatigue Load Model for railway bridges [30] . . . 34
4.1 Fatigue strength curves for riveted details [1] . . . 38
4.2 Representations of effective cross-sectional parameters of corroded (open) sections [3] . . . 41
5.1 Guideline for the fatigue life assessment of existing steel bridges . . . 45
6.1 Overall view of the riveted railway bridge . . . 47
6.2 Bridge drawing - Bane Nor [35] . . . 48
6.3 Cross-sectional axes . . . 49
6.4 Sections of the bridge: (a) Truss girder and (b) Bridge deck . . . 51
6.5 Main truss girder and numbering from SAP2000 . . . 52
6.6 Sections numbering on the bridge deck . . . 52
6.7 Corrosion on structural members: (a) and (b) are from [36], while (c) and (d) from [37] . . . 53
6.8 Corroded cross-sections . . . 54
A.1 Bridge drawing . . . I
B.1 3D modeling of the bridge . . . II
B.2 3D modeling of the bridge . . . III
D.1 Main girder - Top chord (MG-T) . . . VI
D.2 Diagonal truss member (DT) . . . VI
D.3 Vertical truss member (VT) . . . VII
D.4 Main girder - Bottom chord (MG-B) . . . VII
D.5 Stringer (ST) . . . VIII

D.6 Cross girder (CG) IX
D.7 Cross girder (CG-edge) X
D.8 Wind bracing (BR) XI
D.9 Wind bracing (BR-edge) XI
E.1 Train type 1 XIII
E.2 Train type 2 XIII
E.3 Train type 3 XIII
E.4 Train type 4 XIV
E.5 Train type 5 XIV
E.6 Train type 6 XIV
E.7 Train type 7 XV
E.8 Train type 8 XV
E.9 Train type 9 XV
E.10 Train type 10 XVI
E.11 Train type 11 XVI
E.12 Train type 12 XVI

List of Tables

2.1 Mechanical properties of the tested specimens [25] 23
2.2 Tensile and yield strengths for structural steel - Statens Vegvesen [27] 24
2.3 Material stiffness according EN 1993-1-1 25
2.4 Comparison of the mechanical properties from tensile tests and the standards 25
3.1 Riveted joint fatigue strength values and their corresponding number of cycles 30
3.2 Recommended values for partial factors, γ_{Mf} , for fatigue strength [31] 32
3.3 Standard traffic mix with axles ≤ 22.5tonnes (225kN) [32] 35
3.4 Light traffic mix with axles ≤ 22.5tonnes (225kN) [32] 35
3.5 Heavy traffic mix with axles ≤ 22.5tonnes (225kN) [32] 36
4.1 Parameters utilized in the proposed fatigue strength curve of riveted details in corrosive environments 39
4.2 Average values for corrosion parameters A and B, for carbon [33] 42
6.1 Cross-section descriptions and abbreviations [35] 49
6.2 Cross-sectional parameters, provided by SAP2000 50
6.3 Cross-sections and their corresponding numbers in SAP2000 51
6.4 Estimation of the corrosion penetration 54
6.5 Cross-sectional parameters of the corroded cross-sections 55
7.1 Members with fatigue life inferior to 10 years 56
7.2 Case 1 - Standard traffic mix 57
7.3 Case 2 - Light traffic mix 57
7.4 Case 3 - Heavy traffic mix 58
C.1 Fatigue life, < 50 years, of members from the main truss girder IV
C.2 Fatigue life, < 50 years, of members from the bridge deck V
D.1 Cross-section dimensions XII

Abbreviations

D	Damage accumulation factor
CAFL	Constant Amplitude Fatigue Loading
VAFL	Variable Amplitude Fatigue Loading
LM	Load Model
FLM	Fatigue Load Model
EAC	Environment Assisted Cracking
CF	Corrosion Fatigue
SCC	Stress Corrosion Cracking
HE	Hydrogen Embrittlement
HCF	High cycle fatigue
LCF	Low cycle fatigue
ULCF	Ultra-Low cycle fatigue
S-N	Stress-Number of cycles curve of the structural details
MG	Main truss girder
CG	Cross-girder
ST	Stringer

Symbols

Latin letters

A	cross-sectional area
A_{eff}	effective cross-sectional area
C(t)	average corrosion penetration [mm]
E	Young's modulus of material
I	second moment of area
I_{eff}	effective second moment of area of the corroded cross-section
m	negative inverse slope of the fatigue strength curve (S-N curve)
n_i	number of cycles actually undergone by $(\Delta\sigma_{\mathrm{R}})_i$
N_{Ri}	number of cycles that can be done by $(\Delta\sigma_{\mathrm{R}})_i$ before fatigue failure
$N_{f,\mathrm{LCF}}$	number of cycles to fatigue failure of the material at the yield strength, 10 thousand cycles
$N_{f,\mathrm{CAFL}}$	number of cycles at constant amplitude fatigue limit, 5 million cycles
$N_{f,\mathrm{VAFL}}$	number of cycles at variable amplitude fatigue limit, 100 million cycles
t	age of the structure, in years
t_0	time when the first sign of uniform corrosion appeared, in years
W_{el}	section modulus
$W_{el,eff}$	Effective section modulus of the corroded cross-section

Greek letters

$\Delta\sigma$	nominal direct stress range
$\Delta\tau$	nominal shear stress range
$\Delta\sigma_C$, $\Delta\tau_C$	reference stress range value of the fatigue strength (calculated at 2 million cycles)
$\Delta\sigma_D$, $\Delta\tau_D$	constant amplitude stress range value at $N_{f,CAFL}$ number of cycle (fatigue limit)
$\Delta\sigma_L$, $\Delta\tau_L$	stress range value at $N_{f,VAFL}$ number of cycles (cut-off limit)

$\Delta\sigma_{\mathrm{m}}$	mean stress range
σ_{max} , σ_{min}	maximum and minimum applied stress
$\Delta\sigma_{cor}$	stress range for corroded members
γ_{Mf}	the partial safety factor for fatigue strength
γ_{Ff}	the partial safety factor for fatigue loading

1 Introduction

1.1 Background and Motivation

A notable amount of the railway bridges (mainly in Europe and North America) are exceeding 100 years of age [2]. These bridges are mostly made of wrought iron and old structural steel. Replacement of all these bridges will be extremely expensive and practically impossible due to their large number [2]. Rail authorities worldwide are also paying close attention to the remaining lifespan of these bridges [3].

While the bridges have remained largely unchanged, with some maintenance, the traffic load has increased. The recurring traffic loads lead to an accumulation of structural damage, which can result to fatigue failure. Additionally, these bridges are subjected to corrosion due to environmental conditions.

The combination of cycling loading and a corrosive environment leads to a phenomenon known as corrosion fatigue. This combined phenomenon has an aggravating impact on the integrity and safety of bridges compared to corrosion and fatigue applied separately.

To evaluate the fatigue life of components exposed to corrosion fatigue, it is essential to use newly developed fatigue curves (S-N curves) specific to structural elements in corrosive environments. However, these curves have not yet been adopted into standards for fatigue assessment of bridges.

One of the most notable bridge failures is the I-35W Mississippi River bridge in Minneapolis, United States, which occurred in 2007. Both corrosion and fatigue were contributing factors.

1.2 Aim and objectives

The objective of this research is to utilize the newly proposed S-N curve for corroded components, from Adasooriya et al. [1], to estimate the fatigue life of an existing railway steel bridge.

The aims is to compared these results with the Palmgren-Miner damage accumulation method. Then assess the applicability and significance of the proposed curve. Finally, this research intends to develop assessment guidelines based on the findings.

Another objective of this article is to approximate the material properties of the bridge.

The objectives can be divided into parts and classified in sequence.

1. Determine the material properties of century old bridges, especially in Noway, through literature review of past experimental studies.
2. Estimate the fatigue life of an existing steel bridge using the Palmgren-Miner damage accumulation method

3. Estimate the fatigue life of the bridge using the newly proposed formulas
4. Compare the results from both approaches
5. Assess the applicability and significance of the newly proposed fatigue curve.
6. Establish a practical guidelines

1.3 Significance

The recently developed fatigue curves (S-N curves) [1] designed for structural elements in corrosive environments are not yet integrated into bridge assessment standards.

Adasooriya et al. [4] states that Environment-Assisted Cracking (EAC), encompassing corrosion fatigue, is one of the major causes of the degradations of steel bridges and bridge authorities have not properly identified it's effects.

This paper attempt to contribute to the assessment of the applicability and importance of the proposed new method, with the goal of eventually being included into the fatigue assessment code in the future.

1.4 Scope and limitations

This thesis will deal with:

- Direct stress ranges $\Delta\sigma$
- The effect of uniform corrosion (other types of corrosion will still be explained)
- Deterministic approach
- Steel railway bridges with riveted details (connections)

Limitations:

- The effect of temperature on the fatigue life of the structure will not be studied.
- Shear forces and torsional moments will not be considered Item bridges made with material other than steel will not be discussed

1.5 Outline: Thesis structure

Chapter 1: Introduction

The introduction chapter aims to give a comprehensive understanding of the research topic, highlighting the crucial importance of fatigue assessment for existing steel bridges. It outlines the research problem and details the objectives pursued throughout the study.

Chapter 2: Literature review

The "literature review" chapter analyses existing research on relevant topics such as fatigue, corrosion, Environment-Assisted Cracking and structural metals used for bridge construction, the mechanical properties of centuries-old bridges, and riveted connections. This chapter seeks to identify research gaps, inconsistencies, and areas warranting further exploration.

This chapter also aims to determine the material properties of old structural steel used for the construction of bridges. An experimental study will be presented. The results of the experimental study will be compared with values from standards and local guidelines.

Chapter 3: Methodology

The methodology chapter describe the methods and procedures employed to conduct the research, providing a detailed roadmap for the execution of the study. It begins by defining the relevant European standards and local guidelines governing fatigue assessment of steel bridges.

Fatigue design using the Palmgren-Miner method is presented, along with the load models used for fatigue assessment of railway bridges.

Moreover, software employed for bridge modeling and the calculation methodology for the fatigue life are indicated.

Chapter 4: Fatigue life assessment of members in a Corrosive Environment

In this separate chapter, part of the methodology focuses on the approach to estimating the fatigue life of members of the bridge in corrosive environment. It include two main works from Adasooriya et al. [1], [3].

The first research is the newly proposed fatigue strength curves (S-N curves) adapted to riveted details in a corrosive environment. The second research focuses on the estimation of the effective cross-sectional parameters of a corroded bridge member, including the new neutral axis, the new cross-sectional area and the new second moment of area.

Ultimately, this section explained how to use these two papers together to estimate the reduced fatigue

life of the corroded members.

Chapter 5: Assessment guidelines for the fatigue life of existing steel bridges

This chapter attempts to propose a practical guideline for the fatigue life assessment of existing bridges based on the two methods seen before (New S-N curves and Palmgren-Miner damage method)

The guideline is proposed in form of flowchart diagram.

Chapter 6: Case study

The case study chapter provides comprehensive insights into the structural characteristics of the selected bridge and configuration, including geometry, cross-section types, detail category, and corroded sections. It presents all the collected data and assumptions used for the estimation of the fatigue life using both Miner's method and the newly proposed S-N curves.

Chapter 7: Results

The results chapter presents the findings of the fatigue analysis for the case study bridge, including fatigue life estimation for critical members and those simulated with corrosion.

Chapter 8: Discussion

The discussion chapter interprets the fatigue analysis findings considering the research objectives, explaining any deviations and unexpected values through critical analysis and comparison with existing literature.

Chapter 9: Conclusion

The conclusion chapter summarizes the key findings of the research and suggests areas for future work.

2 Literature review

2.1 Fatigue

Fatigue is defined by the Eurocode EN 1993-1-9 as the process of initiation and propagation of cracks through a structural part due to action of fluctuating stress.

According to [5], a study about the cause of damage on steel structures has revealed that in a total of 448 damage cases reported between 1955-1984, 128 of them were bridges. In this 128 bridges, 49 failed due to fatigue, which is 38% of total of bridges that failed.

Siwowski [6] states that most of the steel bridges at that period (1955-1984) were riveted bridges.

In a recent study, 2024, Rajchel and Siwowski [7] confirm that fatigue is one of the most common causes for failure in existing steel railway bridges, especially with a riveted structure.

2.1.1 History of fatigue

The phenomenon of fatigue was first discovered in 1843 by Rankine. He presented a paper to the Institution of Civil Engineers in London about the unexpected breaking of railway axles under cyclic loads, describing the phenomenon as "gradual deterioration" [8].

In the late 19^{th} century, 1858-1870, August Wöhler, a german railway engineer, conducted extensive experiments, including full-scale tests on railway axles, to understand the principles of fatigue. He developed the S-N (stress-number of cycles) approach to fatigue design, which is still widely used today [8]. In fact, the S-N curve is also referred to as the Wöhler curve.

One of Wöhler's significant observations was the existence of a fatigue limit (or endurance limit) for steel materials. This is a stress level below which the material can theoretically endure an infinite number of load cycles without failing. He observed that for steel, this fatigue limit typically occurs at lives greater than 5×10^5 cycles [8].

Wöhler also explored the impact of notches on fatigue life. He demonstrated that the presence of notches significantly reduces the fatigue life of materials, highlighting the importance of minimizing sharp geometrical characteristics in fatigue designs.

Wöhler's work established a fundamental basis for current fatigue analysis and influenced the development of design codes and standards that include fatigue life estimation.

2.1.2 Case histories of bridges failed due to fatigue

I-35W Mississippi River bridge

The I-35W Mississippi river bridge was an 579 m long steel truss arch bridge located in Minneapolis, Minnesota, United States, and was opened in 1967. The bridge collapsed on August 1, 2007, during the rush hour, killing 13 people and over 100 people injured [9]

According to Subramanian [9, p. 32], a 2006 report has documented that the bridge "exhibited several fatigue problems, primarily due to unanticipated out-of-plane distortion of the girders. Numerous fatigue cracks were noted in the approach spans". The report also found that five main truss members were prone to fractures and should have been retrofitted with high performance steel and high strength bolts. It also been noted the presence of several cases of poor weld details, section loss, pitting, flaking, corrosion (including corrosion of expansion bearings), and cracks (many previously drilled out and braced).

Sgt. Aubrey Cosens V.C. Memorial Bridge

The Latchford Bridge was a steel tied arch bridge with a concrete deck, built in 1960, crossing the Montreal River, Canada. It had a span of 110 m and 12 vertical hangers in each arch plane [10].

On January 14, 2003, a truck was crossing the bridge when the northeast part of the bridge deck settled about 2 m [10]. The bridge got closed after that event. This failure is explained in three phases. In total 3 hangers ruptured. The first hanger failed due to fatigue and some years later a second one failed due to fatigue and overload. In 2003, the third hanger failed due to overload and brittle fracture favorised by the cold environment [10].

2.1.3 Fatigue mechanism

Fatigue failure processes are typically described in three stages, each with its own unique characteristics, according to Larsson [11]. This include:

- Crack initiation, resulted by a crack formation in the microstructure of the steel
- Crack propagation, which is the process of crack growth in the material
- Failure, caused by rapid crack growth

Phase 1: Crack initiation

Cracks initiate as a result of plastic deformation caused by tension on grains in the steel [11].

The plastic deformation in the crystal happens when the applied stresses reach their yield point, and this usually begin at notches or stress raisers [11].

Phase 2: Crack propagation

Continuous cyclic loading causes crack propagation, which causes cracks to form into one or more major cracks.

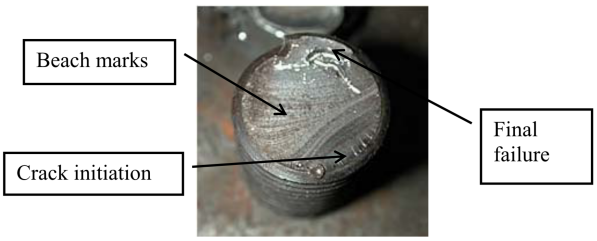

Figure 2.1: Fatigue progress and failure of a bolt [12]

Crack propagation is associated with the phenomenon of "beach marks" in figure 2.1, and leading to the last stage.

Phase 3: Failure

Failure is the last stage of the fatigue mechanism, characterised by rapid growth of the crack, resulting in failure. This occurs when the remaining area of the section can no longer withstand the applied load [11]. There are two principal failure modes: brittle failure, driven by a rapid collapse and ductile failure, characterised by a plastic deformation the the remaining cross-section [11].

2.1.4 Methods for fatigue life evaluations

According to [13], There are three fatigue-life assessment methods typically used in engineering practice, i.e.,

- the nominal stress method, also known as the S–N approach,
- the strain-life method know as the local strain, $(\varepsilon - N)$ approach
- the fracture mechanics-based approach commonly known as the $\frac{da}{dN} - \Delta K$ method

The nominal stress, denoted by S or σ, is used as the load parameter in the S-N approach, so fatigue properties must be calculated in terms of identically defined nominal stress [13].

The local strain-life $(\varepsilon - N)$ approach is based on the analysis of the actual elastic-plastic strains and stresses at the crucial point (such as notches tip), and the local strain ε indicates the load parameter.

The fracture-mechanics-based method necessitates the study of fatigue-crack growth from its starting dimension to the critical size. The Stress Intensity Factor K represents the load parameter, whereas the material fatigue properties are determined by the relationship between the fatigue-crack growth rate $\frac{da}{dN}$ and the stress intensity range ΔK [13].

Nominal stress, is the method that will be utilized in this paper.

2.1.5 Fatigue stresses

Constant and variable stress amplitude

Nominal stress

Nominal stress is estimated based on the general dimensions and applied loads of a structural member, excluding local stress concentrations or discontinuities. It is commonly calculated using simple equations of elastic theory.

Nominal stresses can consist of direct, shear, principal, or equivalent stresses, according to EN 1993-1-9.

Only direct stresses will be considered in this paper.

The direct stresses are composed of axial stresses and bending stress. Axial stresses are caused by axial forces (or loads) and bending stresses are caused by the bending moments. Bending stresses have two components for each axis in a 2D cross section.

$\sigma = \sigma_a + \sigma_b + \sigma_b$
a: axial
b: bending

The complete formula to determine the direct stresses is:

$$\sigma = \frac{N}{A} + \frac{M_{33}}{I_{33}} z_{max} + \frac{M_{22}}{I_{22}} y_{max} \tag{2.1}$$

where

N is the axial (normal) force [N]

A is the cross-sectional area [mm^2]

M_{33}, M_{22} are the bending moments [N.mm]

I_{33}, I_{22} is the second moment of area [mm^4]

z_{max} is the distance from the centroid (neutral axis) to the furthest edge, in the vertical axis

y_{max} is the distance from the centroid (neutral axis) to the furthest edge, in the horizontal axis

The equation can also be written as

$$\sigma = \frac{N}{A} + \frac{M_{33}}{W_{el,33}} + \frac{M_{22}}{W_{el,22}} \tag{2.2}$$

$W_{el,33}$, $W_{el,22}$ are the section modulus $[mm^3]$

The section modulus is a geometric property of a cross-section that indicates the capacity of an element to resist a bending moment, can be expressed as:

$$W_{el,33} = \frac{I_{33}}{zmax} \quad [mm^3]$$

$$W_{el,22} = \frac{I_{22}}{ymax} \quad [mm^3]$$

A high value of section modulus indicates a strong resistance to bending moment.

Fatigue-strength curve or S-N curve

The fatigue strength curve is one of the most important notions in fatigue assessment.

According to EN 1993-1-9, the fatigue strength curve is the quantitative relationship between the stress range and the number of stress cycles to fatigue failure, used for the fatigue assessment of a particular category of structural detail.

The detail category, denoted $\Delta\sigma_c$, is a numerical designation attributed to a type of connection (riveted, bolted, or welded) to indicate its resistance to fatigue load. Figure 7.1 from EN 1993-1-9 displays a list of fatigue-strength curves for several different details categories.

More details about fatigue-strength curve will be found in chapter 3: Methodology.

2.2 Corrosion

Corrosion can be defined simply as the deterioration of steel over time. Revie & Uhlig [14] describe corrosion as the destructive attack of a metal by chemical or electrochemical reaction with its environment. They also mentionned that deterioration caused by physical factors is not referred to as corrosion, but rather as erosion, galling, or wear [14].

2.2.1 Electrochemical process of corrosion

According to [14], the student must be familiar with the principles of chemistry in order to understand the corrosion reactions, since the corrosion processes are mostly electrochemic. The student should also get familiar with the fundamentals of physical metallurgy, as the structure and composition of a metal often describe corrosion behavior [14].

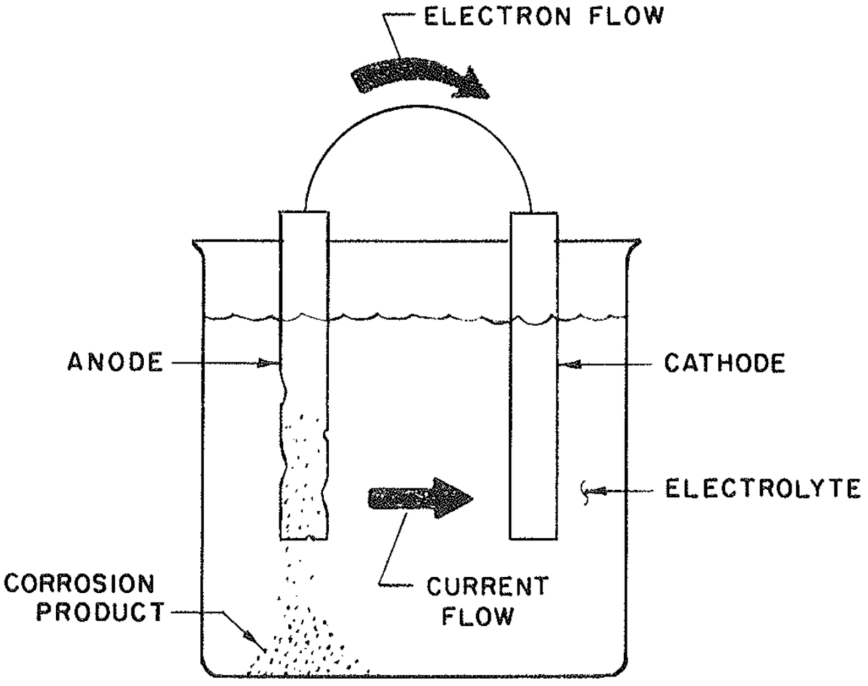

Figure 2.2: Simplified corrosion process: a basic wet corrosion cell [15]

According to [16], the corrosion is easier to explain using a wet corrosion cell like in Figure 2.2, which has four essential components: anode, cathode, electrolyte and electrical connection. In the absence of any one of these components, the corrosion reaction will stop.

Anode: the location where oxidation occurs. The metal corrodes by losing electrons and by forming discrete ions in the solution [17].

$$M \rightarrow M^{z+} + ze^{-}$$

M: the metal

M^{z+}: the metal has a positive charge of z due to the loss of electrons, becoming a metal ion

ze^{-}: number of electrons (negatively charged) lost by the metal atom

M is the metal that is oxidized to form the metal ion (M^{z+}) and releases z electrons in the reaction process.

Cathode: will attract the electrons released by the anode, and consumed by the reactions

$$N^{z+} + ze^{-} \rightarrow N$$

$$2H_2O + O_2 + 4e^- \rightarrow 4OH^- \quad pH \geq 7$$

$$2H^+ + 2e^- \rightarrow H_2 \quad pH < 7$$

N: nitrogen

H_2O: molecules of water

O_2: molecule of oxygen

The equations originate from Tavakkolizadeh and Saadatmanesh [16].

When negatively charged electrons are released from the anode, positive charged ions from the anode metal are released into the electrolyte [15]. These ions will react with other materials to form "corrosion products" [15].

Electrolyte: a solution with sufficient conductivity to allow transfer of ions. On bridges, this electrolyte is usually water [15].

Electrical connection: a connection is necessary between the anodic and cathodic sites for corrosion to occurs. If the anode and the cathode are not made of the same material, a physical connection is necessary for the current to flow and the corrosion to occur [16]

2.2.2 Corrosion mechanism of an iron F_e

The equations are derived from [18] and [17].

Anodic reaction

$$\text{Fe (iron metal)} \rightarrow Fe^{2+} \text{ (ions)} + 2e^- \text{ (electrons)}$$

Cathodic reaction

$$\frac{1}{2}O_2 \text{ (oxygen)} + H_2O \text{ (moisture)} + 2e^- \rightarrow 2OH^- \text{ (hydroxyl)}$$

The ferrous Fe^{2+} and hydroxyl OH^- ions react to form a ferrous hydroxide:

$$2OH^- + Fe^{2+} \rightarrow Fe(OH)_2 \text{ (form of rust)}$$

According to Bayliss and Deacon [18], ferrous hydroxide $Fe(OH)_2$ is a simple form of rust which is unstable and eventually oxidized (i.e., reacts with oxygen) to form the familiar rust, designated as

$Fe_2O_3 \cdot H_2O$. It is the form of rust normally produced in air, natural water, and soils.

2.2.3 Types of corrosion

Kaysser [19] describe the most common forms of corrosion as general corrosion, pitting corrosion, crevice corrosion, galvanic corrosion, and corrosion fatigue.

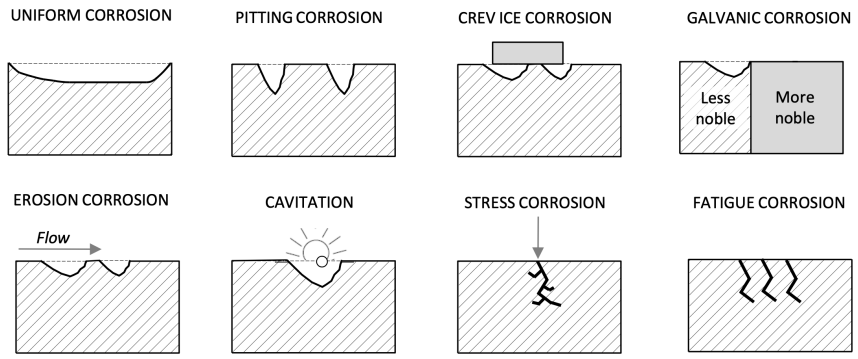

Figure 2.3: The main forms of corrosion [20]

Figure 2.3 illustrates the main types of corrosion. Erosion corrosion and cavitation will not be discussed here.

Corrosion fatigue will be detailed later within the section about Environment-Assisted Cracking (EAC).

1. General corrosion

General corrosion (also known as uniform corrosion) is the thinning of metalwork in a uniform or overall manner [15]. The corrosion is uniformly distributed on the surface. Uniform corrosion can be observed as uniform rust on the surface of a steel bridge [15].

According to [3], in railway bridges with water accumulation, it is common to have general corrosion, especially on the upper side of the bottom flange of wide-flange beams, I-beam stringers, cross-girders, plate girders, built-up sections, and both flanges of built-up sections consisting of riveted angles.

2. Pitting corrosion

Pitting is a type of localized corrosion attack that creates deep, sometimes narrow, penetrations into steel surfaces. It forms when there are chemical or physical changes in the metal, such as defects in steel metallurgy, paint protection flaws, or most frequently, the deposition of foreign material [15]. Pitting can increase stress and lead to failure through cracking [15].

3. Crevice corrosion

Crevice corrosion is a type of localized corrosion that occurs in confined spaces with limited access

to the outside environment [15]. It is caused by variations in the environment inside and outside the crevice, such as oxygen cell or metal ion concentrations. The presence of chloride ions enhances crevice corrosion [15].

4. Galvanic corrosion

Galvanic corrosion, also known as dissimilar metal corrosion, occurs when metals with different compositions come into contact with an electrolyte [15]. The difference in their corrosive potential causes electron flow, with one metal acting as an anode and the other as a cathode.

The metal with the most negative electrode potential (anode) loses electrons and corrodes, whereas the metal with the more positive electrode potential (cathode) remains protected. The corrosion process is driven by electrons that flow from the anode to the cathode through the external circuit.

Anodic	1. Magnesium	8. Nickel	
	2. Zinc	9. Brass	
	3. Aluminum	10. Copper	
	4. Steel	11. Bronze	
	5. Cast Iron	12. Silver	
	6. Lead	13. Gold	
	7. Tin	14. Platinum	*Cathodic*

Figure 2.4: Condensed list of the galvanic series for most common metals [15]

Figure 2.4, the galvanic series illustrates, which metal is protected when two metals are joined. When two metals come together, the more anodic one will be corroded, while the more cathodic one will be protected.

Inspection method: Four of the corrosion types listed above can be observed visually by naked eye.

2.2.4 Effects of corrosion on steel bridges

Kulichi [15] lists four fundamental types of corrosion effects the structural integrity of the bridge, which are loss of section, stress raisers (or stress concentration), unintentional fixity, and unintented movement

1. Loss of section

As the steel member deteriorate over time due to corrosion, it loose thicknesses and lead to multiple geometrical properties reduction. This include the cross-sectional area, cross-sectional centroid, moment of inertia, and torsional and warping constants. The changes are not always linear [4]. These changes of geometrical properties influence the overall stiffness and behaviour of the structure (i.e. stresses, displacements, and dynamic properties) [4].

2. Stress raisers (or stress concentration)

Localised corrosion induce notches or pits that create stress concentration and can initiate cracks [4].

3. Unintentional fixity

Corrosion can block flexible component of the bridge, for example bearing or hinge, and cause the structure to behave differently than intended.

4. Unintented movement

The accumulation of corrosion products (i.e. built up corrosion) on a restrained surface, can generate a high pressure (~ 68 Mpa, according to [15]) that will bend or move a bridge component.

Additionnaly to these for corrosion effects, Adasooriya et al. [4] add the "degradation of material strength".

5. Degradation of material strength

The combined action of some types of corrosion (mostly pitting and crevice) and cyclic loading affects the material and initiates cracks, which tend to reduce fatigue strength. This has the effect of reducing the service life of aging steel bridges.

2.2.5 Factors influencing the rate and progression of corrosion

According to [15], the rate and severity of corrosion depend on environmental conditions, structural details, cleanliness, surface coating, and the maintenance history of the structure. Adasooriya et al. [4] adds to that material of the bridge, inspection procedure and stress levels.

Adasooriya et al. [4] states that factors affecting the corrosion progression can be classified into three main categories: environmental, metallurgical, and structural factors. A "prevention factor" will be added to that.

Structural factors

The structural factors are case-dependent [4]. It can for example be a bridge geometrical details that will collect water. For example a channel section.

Environmental factors

Air pollutants, temperature, pH, and galvanic couple can influence the speed of corrosion. Air polluants can include dissipated oxygen or salt in the air, or acid from gaseous environment [4].

The corrosion rate increases significantly when the pH is <44, and decreases when the pH is >10. Between 4-10, the pH doesn't usually influence the corrosion rate [4]. The maximum corrosion rate for iron and steel happened when the concentration of water is ~ 3,5wt% NaCl, which is close to the

seawater concentration [4].

Metallurgical factors

One of the main metallurgical factor that influence the rate of corrosion of steel is the steel production process, which can be done via an oxygen furnace, open-hearth, Bessemer process, or other processes such as for wrought iron or cast iron [4].

Prevention factor

Prevention factor include cleanliness, surface coating, and stress level. These factors are influenced by the intervention of an external agent.

This leads to the next point, which is corrosion prevention.

2.2.6 Corrosion prevention

Bridge details

It is difficult and costly to change a structural details after a bridge is constructed, but some upgrades can be performed to increase corrosion resistance. For example drilling holes in non-critical locations of members susceptible to accumulate water, to provide drainage. Drip bars can be added to both the top and bottom flanges to prevent water accumulation. Movable and rotating components must be well maintained to prevent them being immobilized.

Cleaning

Bridge cleaning can be a cost-effective way to reduce corrosion of members [15].

The act of cleaning involves removing corrosive deposits, such as salt, atmospheric pollutants, and bird droppings [15].

Bridge cleaning should be scheduled depending on the exposure of the structure to corrosive agents. Areas with high corrosive environment, the cleaning should be performed frequently.

Regular bridge cleaning in dry or semi-dry areas can be as effective as painting in preventing corrosion [15].

Painting and coating

A bridge coating is an important part of corrosion prevention [15]. A proper selection of paint is important and should consider factors such as its corrosion resistance characteristics, cost, ease of application, resistance to wear and cleaning, and availability [15].

Cathodic protection is also a good way of preventing corrosion.

Repair

Repair is based on restoration of the damaged member to its original cross-sectional area [15]. This can be necessary for highly corroded members that could put the safety and integrity of the bridge at risk.

2.2.7 Importance of corrosion

Corrosion is important for three primary reasons: economic, safety and conservation [14].

Conservation

"Conservation" has several applications. Conservation of the structural integrity of the structure, conservation of the environment, conservation of energy (example of pipes transporting water, gas or oil), and the conservation of the human effort to fabricate the structure in the first place [14].

Safefty

Corrosion can put at risk the safety of operational equipment by producing failure, which can result in disastrous consequences [14].

Economic

Economic losses can be classified into types: direct and indirect losses Direct losses include costs due to replacement of corroded elements, painting (or coating), maintenance of cathodic protection systems, use of expensive corrosion-resistant metals and alloys instead of carbon steel,.

Indirect losses might include income loss due to a production system shutdown, loss of corroded non-reparable items, and loss of efficiency from corroded components.

Corrosion cost studies have also been conducted in Australia, the United Kingdom, Japan, and other nations. In each country investigated, the cost of corrosion is around 3-4% of the Gross National Product (GDP) [14], [21]. According to "The world bank" [22], the Gross National Product of Norway was 593,35 billion US dollars, what will be a total of 17,8 billion US dollars if the corrosion cost was 3% of the GDP that year.

2.2.8 Case histories of bridge failures due to corrosion

Several cases of failures of bridges due to corrosion can be noted. Adasooriya et al. [4] have established a summary table of several bridges failure caused by corrosion, including:

- One of the most know, Mianus River Bridge, in Greenwich, built in 1958 and failed in 1983 (i.e. 25 years later). The failure occurred due to the accumulation of corrosion products in a washer, which caused a misalignment of the hanger. The stress level at the end of the pin was increased due to this misalignment, ultimately leading to a fatigue crack. The inspections failed to detect the

change in misalignment and the effect corrosion on the bridge since that part was not part of the regular inspections [4].

- Silver Bridge, built in 1928 and failed in 1967 (i.e. 39 years later). The bridge was an eyebar suspension bridge type. The failure occurred due to cracks at the pin hole due to corrosion in an eye bar [4]. According to Choudhury and Hasnat [23], the bridge collapsed without warning on December 15, 1967 during the evening rush hour, when it was was crowded with heavy traffic, and resulted in the loss of 46 lives and nine injuries.
- Kinzua Bridge, Pennsylvania, built in 1882 and failed in 2003 (i.e. 121 years later). This bridge failed due to corrosion on anchor bolts holding the bridge to its foundations [4].

2.3 Environment-Assisted Cracking

Environment-Assisted Cracking (EAC) is the degradation of metal structures, such as steel bridges, caused by a combination of mechanical stress and corrosive environment. The primary distinction between normal corrosion and EAC is the presence of stresses in EAC.

There are three conditions for EAC to occur [24]: a susceptible material, an appropriate environment and a sufficient tensile stress

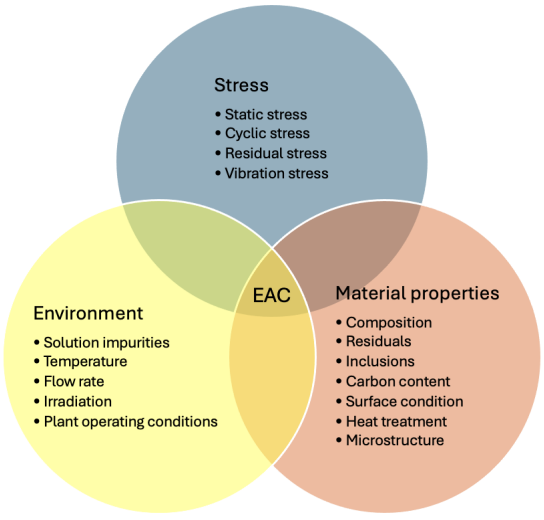

Figure 2.5: Main conditions for EAC to occur [24]

EAC includes three major types, according to [4], [24] : Stress Corrosion Cracking (SCC), Hydrogen Embrittlement (HE), and Corrosion Fatigue (CF).

Research gap

Researchers continue to highlight the importance of additional research on EAC due to the combined effect of the inherent nature of corrosion and unpredictable loading behaviour, Adasooriya et al. [4].

2.3.1 Corrosion Fatigue (CF)

Kulichi et al. [15] define CF as a fatigue-type cracking of metal caused by repeated or fluctuating applied stresses in a corrosive environment.

Corrosion fatigue is distinguished from regular corrosion by the presence of a corrosive environment.

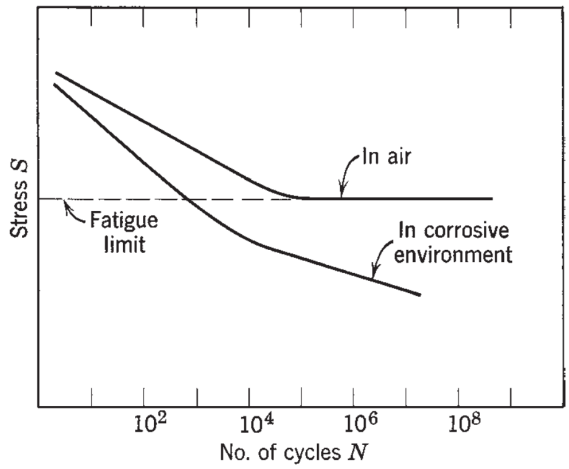

Figure 2.6: S-N curve for steels subjected to cyclic stress [14]

CF considerably decreases the fatigue life of the affected member as compared to its life in a non-corrosive environment.

From figure 2.6, it can be observed that, without a corrosive environment, there an endurance limit or fatigue limit in which the stresses below this limit will not affect the fatigue life of the concerned member. On the other hand, in corrosive environments, even low stresses can contribute to reducing the fatigue life of the affected member.

Occurrence

Corrosion fatigue on steel bridges only affects fatigue-sensitive members in corrosive environments.

Mechanism

According to Kulichi et al. [15], the mechanism of corrosion fatigue is similar to stress corrosion cracking, with corrosion generating stress concentrations that initiate cracks.

Usually after the initiation, the crack will propagate until failure occurs.

Figure 2.7: Corrosion-fatigue crack in mild steel sheet (250x) [14]

Inspection method

Corrosion fatigue must be checked by microscopic examination [15].

2.3.2 Stress Corrosion Cracking (SCC)

Stress corrosion cracking is a type of cracking that occurs when tensile stress (either residual or applied) occurs at the same time as a corrosive environment [15]. Residual stresses result from fabrication processes.

The cracks can be intergranular (around grains) or transgranular (across grains), but they typically occur perpendicular to the member stress [15]. Stress corrosion cracking is characterized by a brittle fracture in a metal that is otherwise ductile.

The stress-corrosion cracking process generally consists of three stages [14]:

- Generation of the environment that causes S.C.C
- Initiation of S.C.C
- Propagation until failure occurs

2.3.3 Hydrogen Embrittlement (HE)

Hydrogen embrittlement, according to [15], is a loss of ductility in a metal caused by the absorption of hydrogen.

According to [4], hydrogen embrittlement (HE) can be classified into two categories:

- Internal hydrogen embrittlement, which occurs because of preexisting hydrogen in the material matrix.
- Hydrogen environment embrittlement, which occurs when hydrogen is picked up from the environment.

Steels containing hydrogen are vulnerable to HE [4]. When carbon steel is heated to generate martensite, it undergoes hydrogen cracking [4].

2.4 Structural metals for bridges

Early 19^{th} century, metal bridges were primarily constructed from cast iron or puddle iron (also known as wrought iron), according to Moi [25]. However puddle iron provided more advantages than cast iron such as increased ductility, due to its lower carbon content, which can lead to less likely brittle failures.

By the end of 19^{th}, puddle iron was replaced by the mild steel, which provide better characteristic, such as such as greater weldability and strength [25]. Therefore, mild steel became the most used metal in bridge construction in the begining of of 20^{th}.

According to Larsson [11], the first metal bridge is named "Ironbridge", and was built between the years 1777-1781 over the river Severn at Coalbrookdale, UK.

The bridge was built to demonstrate the potential of using this new material [11]. Due to the heaviness of the material, the use of iron was abandoned and the first steel bridge was built in Sweden in 1846 [11].

2.4.1 Cast iron

According to [19], Cast iron is characterised by their high carbon content, over 2 %. Due to theirs high carbon contents, the final product (i.e. shape) could be achieved only by pouring the molten metal into forms (i.e frame). After poured into the molds (i.e. frame), the molten metal can progressively cools and solidifies.

Cast iron has advantages such as, wear resistance, damping abilities, and vibrations and noise absorption [19]. The disadvantages of cast iron is that it is brittle, has a low impact and shock resistance, and it's

not suitable for welding due of its high carbon contents, which can result to brittle cracks in and around welded join [19].

2.4.2 Puddled iron (or Wrought iron)

Puddled iron is characterised by a low carbon content but with high amounts of phosphor and nitrogen, which make it brittle and accelerate the ageing process [19]. The microstructure is non-homogeneous because to sulphide and oxide inclusions produced during the manufacturing process. This resulted in anisotropy of the material, which is particularly weak in the thickness direction [19].

2.4.3 Mild steel (steel)

These steels have experienced major improvements, particularly in strength characteristics, making them similar to modern standards such as S235 [25].

Mild steel from the 19^{th} century are low-carbon steel ($< 2\%$) produced by blast process (Bessemer or Thomas process) or hearth process (Siemens-Martin process) [5].

Mild steel from the 20^{th} century are low-carbon ($< 2\%$), low-alloyed steel manufactured in the late 19^{th} and early 20^{th} centuries utilizing the Thomas or Siemens-Martin processes [5]. Depending on the level of deoxidation, the steels can be un-killed (rimmed), semi-killed, or killed.

- Rimmed (un-killed) steel is minimally deoxidized (oxygen removed), resulting in a pure iron rim and porous core.
- Semi-killed steel is partially deoxidized, resulting in qualities miday between rimmed and killed steel.
- Killed steel is completely deoxidized, producing homogenous, high-quality steel with no gas-related flaws.

2.5 Mechanical properties of century-old railway bridges

There is a lack of information about the material properties of the steel used in bridge construction in the beginning of the 20^{th} century and before, in Norway. Several steel bridges are aged, reaching 100 years, and still in service in Norway.

2.5.1 Experimental study on an old bridge in Norway

To compensate for the lack of documentation on the material properties of century-old steel bridges in Norway, Per Kristian Moi [25] has conducted an experimental examination on elements from a steel railway bridge built in 1908 in Norway

His objective was to analyse the material composition and mechanical properties of the collected elements from the bridge and compare the results with an current standardized steel S235.

The relevance of this study lies in the fact that the elements tested come from a particular period of time and country, as the bridge that will be examined later in the case study, the "Bridge Above Todøla".

Per Kristian Moi [25] has performed multiple experiments, including:

- Tensile tests to assess the mechanical properties
- Spectroscopy (energy-dispersive x-ray spectroscopy) to determine the chemical composition of a beam element

The tensile test was performed with six specimens at room temperature, using a Zwick Roell tensile strength machine. Two of the specimens had three samples and the four others had four samples each. The test specimens were fabricated using Computer Numerical Control (CNC) machining to meet the specifications of the standard ISO 6892-1:2019. One important specification was the thickness to be greater than 3 mm [25].

ISO 6892-1:2019 is a standard that describes the procedure for testing the tensile strength of metallic materials and defines the mechanical properties that can be estimated at room temperature.

According to Per Kristian Moi [25], prior the realization of the test, the specimens were examined for any potential cracks or discontinuities. Also, the thickness and the gauge length have been measured and checked to follow the specifications.

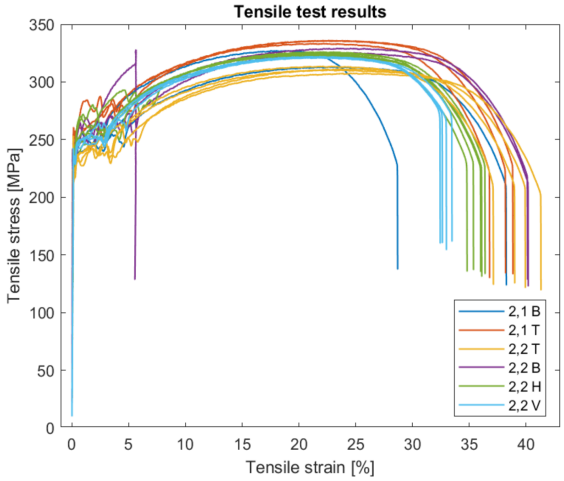

Figure 2.8: Results of the tensile tests of all specimens [25]

Figure 2.8 is a Stress-Strain diagram showing the specimen's behavior during tensile test. According to Per Kristian Moi [25], three tests were found to be invalid, with two of them showing significant

deviation from the general trend. Despite the presence of exceptions, a general trend could be observed, indicating a relatively consistent material property across different locations of the beam.

Table 2.1: Mechanical properties of the tested specimens [25]

Specimen names	Young's modulus E [Mpa]	Yield strength $R_{p0.2}$ (or f_y) [Mpa]	Tensile strength R_m (or f_u) [Mpa]
2,1 T	199	241	335
2,1 B	200	223	320
2,2 T	198	219	311
2,2 V	197	229	321
2,2 H	203	234	324
2,2 B	201	224	327
Mean	200	229	323
95% characteristic value	**189**	**218**	**311**

Table 2.1 is established using the Table 14 in Per Kristian Moi [25] thesis research.

The actual mechanical properties of the elements of the bridge are considered to be "95% of the mean values", know also as "95% characteristic values" . Thus

- Young's modulus E = 189 Gpa,
- Yield strength f_y = 218 Mpa,
- Tensile strength f_u = 311 Mpa

The names of the specimens include numbers and a letter that specify where the specimen was taken from the beam.

2,1 T : means "Top flange of the Beam 2, at location 1". See **Figure 2.9** to see the locations
H and V : specimens extracted from the web
B : means bottom flange

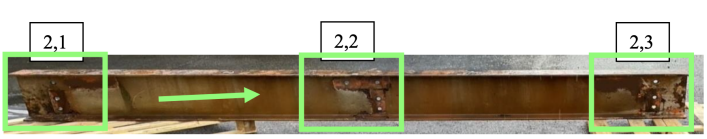

(a) Detached beam from the bridge

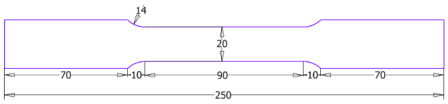

(b) Measurements [mm] of the sample used for tensile tests

Figure 2.9: Beam from the bridge and the sample measurements for tensile tests [25]

Figure (2.9a), illustrates the different location on the beam. The beam is named beam 2, and the green squares show the three different locations, named 1,2 and 3.
Location 1 corresponds to the left end of the beam, location 2 corresponds to the center , and location 3 corresponds to the right end.

2.5.2 Recommended values from standards and local guidelines

This section deal with recommended mechanical properties from the Eurocode and local guidelines in Norway.

The concerned standard is the EN 1993-1-1, which provides nominal values of material properties, such as E, G, and υ, to be adopted as characteristic values in design calculations.

The relevant local guidelines about bridges is Norway are provided by Statens Vegvessen, or in english the "Norwegian Public Roads Administration". Statens Vegvesen is the government agency responsible for public roads, including bridges, tunnels and ferry transportation in Norway.

Guidelines:

- V412: Load capacity classification of bridges, loads [26]. Translated from the norwegian "Bæreevneklassifisering av bruer, laster"
- V413: Load capacity classification of bridges, materials [27]. Translated from the norwegian "Bæreevneklassifisering av bruer, materialer"

The guideline V413 from Statens Vegvessen propose values for mechanical properties of old steel material used in bridge construction.

The table below separate two period of time, bridges buitls before of after 1920.

Table 2.2: Tensile and yield strengths for structural steel - Statens Vegvesen [27]

Age	Steel quality	Tensile strength	Yield strength
		f_u [N/mm^2]	f_y [N/mm^2]
Pre 1920	All steel	350	220
After 1920	St. 37	370	235
	St. 42	420	255
	St. 44	440	265
	St. 52	520	345

As the case study bridge in this thesis if built in 1906, the corresponding material properties is: yield

strength = 220 Mpa and tensile strength = 350 Mpa.

The density of the steel is defined in the guideline V412 [26, Section 4.1.1].
Steel density $\gamma = 77\ [kN/m^3]$

According to V413 [27, Section 2.2], the capacity check is performed according to NS-EN 1993-1-1 [28] and NS EN 1993-2 [29], with subsequent material factors and material strengths.

The section 3.2 EN 1993-1-1 is about structural steel material. According to EN 1993-1-1, the nominal values of material properties given in that section should be adopted as characteristic values in design calculations. That section also provide nominal values for yield strength f_y and ultimate strength f_u, Table 3.1, for unknow steel properties.

However, it's the material stiffness, known also as Young's modulus, or elastic modulus that is the interest.

Table 2.3: Material stiffness according EN 1993-1-1

Material parameters		**Reference**
Young's modulus	$E = 210\ 000\ [N/mm^2]$	EN 1993-1-1 , Section 3.2.6 [28]
Shear modulus	$G = \frac{E}{2(1+\upsilon)}$ $G = 81\ 000\ [N/mm^2]$	EN 1993-1-1 , Section 3.2.6 [28]
Poisson's ratio	$\upsilon = 0,3$	EN 1993-1-1 , Section 3.2.6 [28]

2.5.3 Comparison of material properties

On Table 2.4 below, the material properties determined by Moi [25] are compared to the recommended values from the Eurocodes.

Table 2.4: Comparison of the mechanical properties from tensile tests and the standards

	Yield Strength f_y [Mpa]	Tensile Strength f_u [Mpa]	Young's modulus E [Mpa]
Recommended values from V413 (guideline) and Eurocode	220	350	210 000
Tensile test of bridge elements	218	311	189 000
Reduction (%)	0,9 %	11,1 %	10 %

The yield strength observed by Moi [25] is very close to the recommended value from V413, with a difference less that 1 %. The values of Tensile Strength and Young's modulus have a higher differences, with a difference of about 10 %.

2.6 Riveted connections in bridges

A riveted connection is a method of joining two or more plates together, using a rivet. It consists of inserting a rivet through pre-drilled holes in the concerned plates and then hammering the opposite end of the rivet to form a second head.

As the rivet cools and contracts, it generates a compressive force known as "clamping force", which effectively joins the plates.

A rivet is a mechanical fastener used to join materials together (similar to a bolt). It is composed of a shank and a head on one end. The shank is the cylindrical shaft (typically long). The head is on one end of the shaft. The head can have different forms (such as flat, round, countersunk, or pan heads).

Process:

- Holes are drilled into the plates to be joined.
- A hot rivet is inserted through the aligned holes. The rivet is heated to a high temperature (~1000°C) to make it more malleable.
- The exposed end of the rivet shank is deformed by hammering to create a second head.
- As the rivet cools, it contracts, creating a clamping force that holds the materials tightly together.

Although the riveting described above is hot riveting, it is important to note that cold riveting also exists. The majority of old riveted bridges are built with hot rivets.

Riveting was widely used to assemble metal structures, especially civil engineering structures such as bridges, according to Larsson [12]. Nowadays, riveting is mostly used in the aeronautical sector [12].

3 Methodology

This methodology section is focused on both European standards related to fatigue design and load models for railway bridges, with a focus on Miner's damage accumulation model.

3.1 European standards for bridge design and fatigue life assessment

Several Eurocodes are somehow including in the fatigue design for bridges.

Here is an illustration below.

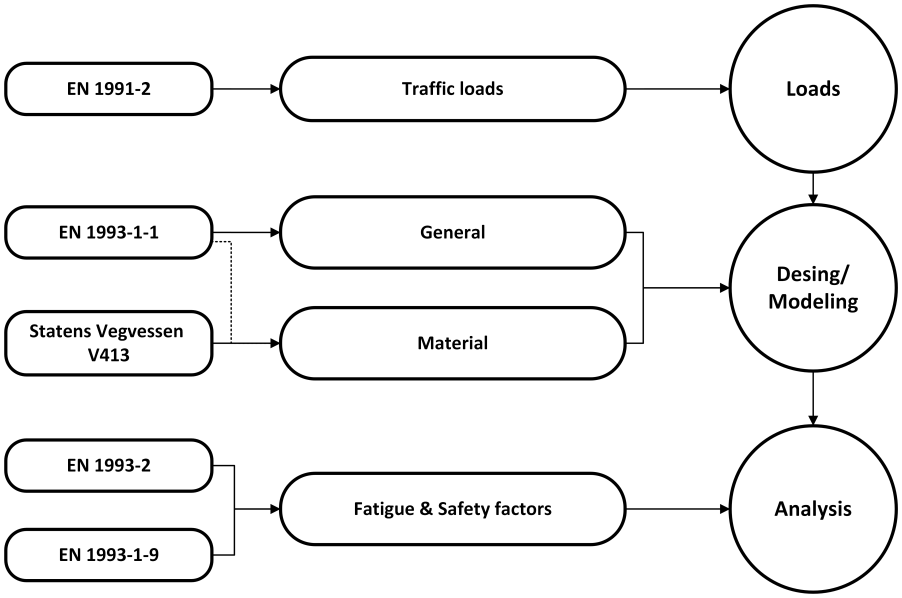

Figure 3.1: Standards and guidelines used for fatigue assessment in this paper

The figure 3.1 about standard related to fatigue design is inspired by [30].

V413, is a Norwegian local guideline for material properties of existing bridges.

3.1.1 EN 1990: Basis of structural design

The European Standard EN 1990:2002 establishes the principles and requirements for the safety, serviceability, and durability of structures and describes the basis for their design and verification. It provides guidelines for structural reliability and is intended to be used in conjunction with other Eurocodes (EN 1991 to EN 1999).

EN 1990 stipulates that monumental building structures, bridges and other civil engineering structures are classified as "category 5", and have to be design for a working life of 100 years.

3.1.2 EN 1991-2: Actions on structures - Traffic loads on bridges

EN 1991-2:2003 is a part of the Eurocode 1 series, which provides guidelines and regulations for actions on structures. This particular part, Part 2, focuses on traffic loads on bridges, covering vehicle bridges (road and railway) and footbridges.

Two primary sections of this standard are crucial when it comes to railway bridges.

- Section 6: "Rail traffic actions and other actions specifically for railway bridges"
- Annex D: "Basis for the fatigue assessment of railway structures"

Section 6 of EN 1991-2 focuses on the actions due to rail traffic on railway bridges, including static and dynamic effects of rail traffic loads. It also introduces load models such as Load Model 71 for standard rail traffic, as well as SW/0 & SW/2 for continuous and heavy rail traffic. The section also outlines the consideration of dynamic factors.

The load models will be detailed in Chapter 3.3.

Annex D of EN 1991-2 defines the general design method for fatigue assessment and specifies the train types to be considered in fatigue analysis.

3.1.3 EN 1993-2: Design of steel structures - Steel Bridges

EN 1993-1-9:2005 is a part of the Eurocode 3 series, which provides a comprehensive framework for the design of steel structures. This "part 2" deal with design of steel bridges.

Chapter 9 in EN 1993-2 is dedicated to fatigue, and provides:

- Additional requirements for fatigue assessment
- The partial factor for fatigue loads shall be taken as γ_{Ff}
- Fatigue assessment procedures such as the damage equivalence factor λ

EN 1993-1-9 states that fatigue assessments for railway bridges should be carried out for all structural elements.

3.1.4 EN 1993-1-9: Design of steel structures – Fatigue

EN 1993-1-9:2005 is also a part of the Eurocode 3 series, and it focuses on the assessment of fatigue in steel structures, ensuring safety and durability under cyclic loading conditions.

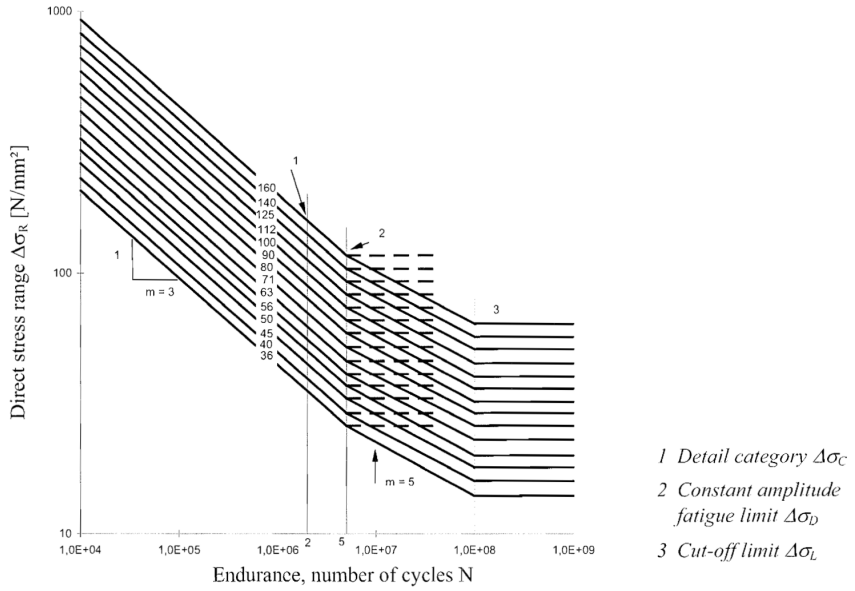

Figure 3.2: Fatigue strength curves for direct stress ranges [31]

The fatigue strengths, figure (3.2), are represented by S-N curves (Stress vs. Number of cycles). The graph plots the stress range ($\Delta\sigma$) on the vertical axis against the endurance (number of cycles, N) on the horizontal axis. These curves correspond to specific detail categories, indicating the fatigue strength for different constructional details.

The detail category ($\Delta\sigma_C$) represents the fatigue strength at 2 million cycles (N = 2.10^6).

The constant amplitude catigue limit (i.e. CAFL, or $\Delta\sigma_D$) represents the stress range below which no fatigue damage is expected under constant amplitude loading.
The cut-off Limit ($\Delta\sigma_L$) represents the stress range below which the stress cycles do not contribute to fatigue damage. Only applies in non-corrosive conditions.

Observations: The curves show that the allowable stress range decreases as the number of cycles increases. Both axes are on a logarithmic scale, reflecting the wide range of stress cycles and stress ranges.

The slopes of the curves are often indicated as m = 3 or m = 5.

For Riveted connections, the detail category is usually considered $\Delta\sigma_C$ = 71 Mpa by the Eurocodes.

Table 3.1: Riveted joint fatigue strength values and their corresponding number of cycles

	Stress range [Mpa]	Number of cycles of associated
Detail Category ($\Delta\sigma_C$)	71	2.10^6
Constant Amplitude Fatigue Limit ($\Delta\sigma_D$)	52,33	5.10^6
Cut-off Limit ($\Delta\sigma_L$)	28,73	100.10^6

$\Delta\sigma_D$ and $\Delta\sigma_L$ were determined using the equations (3.1) and (3.2), respectively.

$$\Delta\sigma_D = \left(\frac{2.10^6}{N_R}\right)^{\frac{1}{3}} \cdot \Delta\sigma_C \quad = 0,737 \cdot \Delta\sigma_C$$

$$\Delta\sigma_L = \left(\frac{5.10^6}{N_R}\right)^{\frac{1}{5}} \cdot \Delta\sigma_D \quad = 0,549 \cdot \Delta\sigma_D$$

Determination of the corresponding number of cycles to failure N_R

The number of cycles N_R can be calculated according to the following formulas:

if $\Delta\sigma_R \geq \Delta\sigma_D$

$$N_R = \left(\frac{\Delta\sigma_C}{\Delta\sigma_R}\right)^3 \cdot 2.10^6 \tag{3.1}$$

if $\Delta\sigma_D \geq \Delta\sigma_R \geq \Delta\sigma_L$

$$N_R = \left(\frac{\Delta\sigma_D}{\Delta\sigma_R}\right)^5 \cdot 5.10^6 \tag{3.2}$$

if $\Delta\sigma_R < \Delta\sigma_L$

$$N_R \rightarrow \infty \text{ (infinity)} \tag{3.3}$$

where

m is the slope of the S-N curve m = 3 ; 5

$\Delta\sigma_C$ is the detail category

N_R is the corresponding number of cycles to fatigue failure. Said differently, it's the number of cycles that $\Delta\sigma_R$ can handle without failure.

$\Delta\sigma$ is the calculated stress range

$\Delta\sigma_R$ is the calculated stress range which includes the partial factors for fatigue (γ_{Ff} & γ_{Mf})

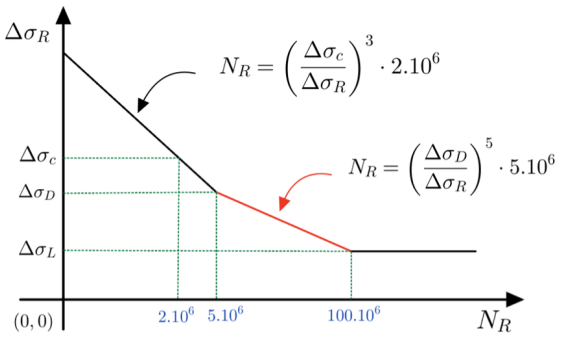

Figure 3.3: Fatigue strength curve with the reference stress ranges

Figure 3.3 gives a visual representations on which condition to use which N_R formula. The top linear black line correspond to the stress ranges superior to $\Delta\sigma_D$ The middle red linear line correspond to the stress ranges inferior to $\Delta\sigma_D$ and superior to $\Delta\sigma_L$. And the bottom straight line correspond to the cut-off limit, where stress ranges below this line will not affect the fatigue damage.

Stress ranges and partial safety factors

$$\Delta\sigma = \sigma_{max} - \sigma_{min} \tag{3.4}$$

$$\Delta\sigma_R = \gamma_{Mf} \cdot \gamma_{Ff} \cdot \Delta\sigma \tag{3.5}$$

where

γ_{Mf} is the partial factor for fatigue strength (EN 1993-1-9: Table 3.1)

γ_{Ff} is the partial factor for fatigue loading (EN 1993-2: 9.3)

The recommended value for γ_{Ff} = 1,0

Table 3.2 below, derived from EN 1993-1-9: Table 3.1, shows the recommended partial factors used in fatigue verification calculations. The partial factor is used to adjust the stress ranges (by increasing it) or the fatigue strengths (by reducing it) to ensure an acceptable level of reliability in fatigue design.

Table 3.2: Recommended values for partial factors, γ_{Mf} , for fatigue strength [31]

Assessment method	Consequence of failure	
	Low consequence	High consequence
Damage tolerant	1,00	1,15
Safe life	1,35	2,00

Assessment method

- **Damage tolerant approach:** This approach is designed to ensure that the structure can resist some damage while performing appropriately with regular inspections and maintenance.
- **Safe life approach:** With this approach, the structure is ensured to function without significant damage for its intended life, without the need for regular inspection specifically for fatigue damage.

Consequences of failure

- **Low consequence of failure:** for members with a minor impact on the bridge when they failed. Therefore, the partial factor has a lower value.
- **High consequence of failure:** for members with a high impact on the bridge when they failed. Therefore, the partial factor is more significant.

3.2 Fatigue design with the Palmgren-Miner damage accumulation method

Palmgren-Miner rule, also known as the Miner's Rule or the Palmgren-Miner linear damage rule, is a principle used to predict the fatigue life of a component subjected to repeated loading.

The idea behind Miner's Rule is to calculate the damage ratio for each type of loading cycle and then sum up these ratios to determine if the total cumulative damage exceeds a critical threshold.

The total (accumulated) damage is defined as:

$$D = \frac{n}{N} \tag{3.6}$$

Thus

when $n \leq N \Rightarrow D \leq 1$, no fatigue failure will occurs

when $n = N \Rightarrow D = 1$, fatigue failure will occurs

The rule assumes that failure occurs when the cumulative damage reaches 100% , i.e. D = 1.0.

$$D = \sum_{i=1} D_i \quad \leq 1,0 \tag{3.7}$$

Or

$$D = \frac{n_1}{N_1} + \frac{n_2}{N_2} + \frac{n_3}{N_3} + \ldots = \sum_{i=1}^{n} \frac{n_i}{N_i} \quad \leq 1,0 \tag{3.8}$$

Where

D is the accumulated damage

n_i is the number of cycles completed

N_i is the number of cycles to failure

The number of cycles to failure N_i for a given stress range $\Delta\sigma_{\mathrm{i}}$ can be calculated similarly as seen previously within the paragraph on EN 1993-1-9: 2005.

$$N_i = 2.10^6 \cdot \left(\frac{\Delta\sigma_{\mathrm{C}}}{\Delta\sigma_{\mathrm{Ri}}}\right)^3 \tag{3.9}$$

$$N_i = 5.10^6 \cdot \left(\frac{\Delta\sigma_{\mathrm{D}}}{\Delta\sigma_{\mathrm{Ri}}}\right)^5 \tag{3.10}$$

$$N_i \rightarrow \infty \tag{3.11}$$

where

Equation (3.9) is applicable when $\Delta\sigma_{\mathrm{Ri}} \geq \Delta\sigma_{\mathrm{D}}$

Equation (3.10) is applicable when $\Delta\sigma_{\mathrm{D}} \geq \Delta\sigma_{\mathrm{Ri}} \geq \Delta\sigma_{\mathrm{L}}$

Equation (3.11) is applicable when $\Delta\sigma_{\mathrm{Ri}} < \Delta\sigma_{\mathrm{L}}$

$\Delta\sigma_{\mathrm{Ri}} = \gamma_{\mathrm{Mf}} \cdot \gamma_{\mathrm{Ff}} \cdot \Delta\sigma_{\mathrm{i}}$

3.3 Fatigue Load Models for the cumulative damage method

Load models are defined in Eurocode EN 1991-2 and serve as the basis for defining rail traffic actions.

The load models defined in this section do not represent actual loads. They have been selected so that their effects, with dynamic enhancements taken into account separately, represent the effects of service

traffic [32].

According to Al-Emrani and Aygül [30], the load models used for fatigue verification of railway bridges can be classified into two main groups based on fatigue assessment methods.

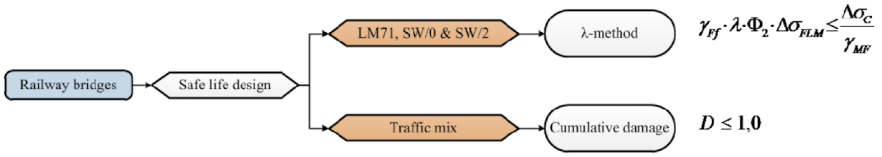

Figure 3.4: Fatigue Load Model for railway bridges [30]

The fatigue assessment of railway bridges is performed according to the “safe life design” approach. The safe life method is meant to ensure that a structure will perform satisfactorily for its design life without the need for regular in-service inspection for fatigue damage. The safe life method should be applied in cases where local crack formation in one component could rapidly lead to failure of the structural component or structure [31].

Unlike the situation for road bridges, an ’infinite life design’ approach of railway bridges would result in an extreme and uneconomic design, according to [30].

Category 1:

This category is intended for fatigue verification using the simplified λ-coefficient approach. This include the fatigue load model 71 (FLM 71), the fatigue load model SW/0 (FLM SW/0) and the fatigue load model SW/0 (FLM SW/2), listed in section 6 of EN 1991-2.

Category 2:

This category is intended for fatigue verification using the damage accumulation concept based on the Palmgren-Miner rule. The fatigue life of structures, using this fatigue load model, must be calculated on a basis of three "traffic mixes", according to EN 1991-2.

A "traffic mix" is a group of various types of trains, where each train have specific daily frequency and its own characteristics. Trains are classified according to several characteristics such as, the type (freight or passenger), the axle loads, the axle spacing, the lengths, and the speeds. Traffic mixes attempt to represent real-life traffic conditions that the bridge could encounter.
Appendix E provides more characteristics details for each train type.

The three traffic mixes are "standard traffic mix", "light traffic mix", and "heavy traffic mix". These traffic mixes are based on a traffic volume of 25 million tonnes annually [32].

3.3.1 Standard traffic mix

The standard traffic mix has the most diverse types of trains, with a total of 8 train types, and 67 trains crossing the bridge every day.

Table 3.3: Standard traffic mix with axles ≤ 22.5tonnes (225kN) [32]

Train type	**Number of trains/day**	**Mass of train** ***[tonnes]***	**Traffic volume** ***[10^6. tonnes/year]***
1	12	663	2,90
2	12	530	2,32
3	5	940	1,72
4	5	510	0,93
5	7	2160	5,52
6	12	1431	6,27
7	8	1035	3,02
8	6	1035	2,27
	67		24,95

3.3.2 Light traffic mix

The light traffic mix consists of four types of trains, with a total of 207 trains crossing the bridge each day. This traffic mix has the highest daily train frequency.

Table 3.4: Light traffic mix with axles ≤ 22.5tonnes (225kN) [32]

Train type	**Number of trains/day**	**Mass of train [t]** ***[tonnes]***	**Traffic volume** ***[10^6. tonnes/year]***
1	10	663	2,4
2	5	530	1,0
5	2	2160	1,4
9	190	296	20,5
	207		25,3

3.3.3 Heavy traffic mix

The heavy traffic mix consists of four types of trains, with a total of 51 trains crossing the bridge each day.

Table 3.5: Heavy traffic mix with axles ≤ 22.5tonnes (225kN) [32]

Train type	**Number of trains/day**	**Mass of train [t]** ***[tonnes]***	**Traffic volume** ***[10^6. tonnes/year]***
5	6	2160	4,73
6	13	1431	6,79
11	16	1135	6,63
12	16	1135	6,63
	51		24,78

These three traffic mixes will be used in the case study for the fatigue life estimation of the bridge.

Applicability of the load models: Theses load models are exclusively applied to rail traffic on the standard track gauge and wide track gauge European mainline network, according to EN 19991-2:2003 [32]. This means that these load models do not apply to other type of tracks, including narrow-gauge railways, tramways and other light railways, preservation railways, rack and pinion railways, and funicular railways [32].

3.4 Methodology used for modeling and structural analysis

Few software were used during this analysis and the estimation of the fatigue life.

SAP2000 for the bridge modeling and the moving load analysis

The modeling and structural analysis were performed using SAP2000. The steps were as follows:

- Create the shape of the bridge, designed the built-up cross-sections and assigned them to the corresponding location in the bridge
- Created the trains loads and applied them to the paths
- Run the analysis to obtain the forces [N] and bending moments [$N.m$] applied to every element of the bridge

Afterwards, these forces and bending moments were sent to Excel for further calculations.

SAP2000 is a civil engineering software, developed by Computers and Structures, Inc. (CSI). It used for the analysis and design of any type of structural system. The software supports several types of analysis, including static, and dynamic, and can execute linear and nonlinear analyses.

Excel for manual calculations

Excel was used for manual calculations, including the calculations of the nominal stresses, the number of cycles to failure N_R, the damage accumulation D, and finally the fatigue life of elements.

AutoCAD for the design of corroded cross-section

The software allows users to easily design discontinuous or asymetric shapes. It is less restrictive compared to SAP2000.

It provide cross-sectional parameters including the cross-sectional area, the center of gravitation, and the second moment of area. The steps were as follows:

- Design the overall cross-section
- Eliminate thicknesses associated with the uniform corrosion
- Compute the effective parameters (z_{max}, y_{max}, A_{eff} I_{eff}).

4 Fatigue assessment of bridges in corrosive environment

4.1 Proposed fatigue strength for riveted details in corrosive environment

A stress-life curve formula to estimate the fatigue life of riveted bridges situated in corrosive environment has been proposed by Adasooriya et al. [1].

The corrosive parameters used to establish the S-N curve below, figure 4.1, were determined based on corrosion fatigue testing results of various steel specimens in air, fresh water, and seawater.

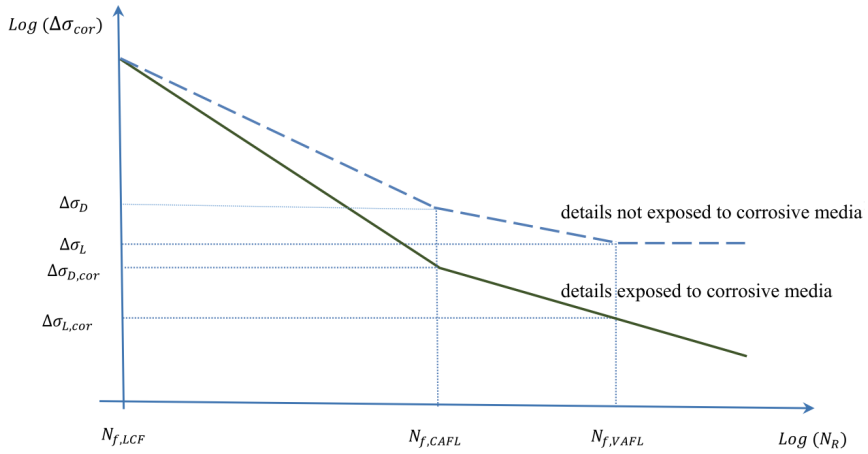

Figure 4.1: Fatigue strength curves for riveted details [1]

Figure 4.1 illustrates two fatigue strength curves for riveted details: one for a details not exposed to corrosive environment and the other for a details exposed to corrosive environment.

The blue dotted line represent the S-N curve of a riveted details not exposed to a corrosive environment. It is typically identified as a trilinear S-N curve, with the presence of a constant amplitude fatigue limit $\Delta\sigma_D$ and a cut-off limit $\Delta\sigma_D$ where the stress ranges below that will not affect the fatigue life. It's the same curve as from the Eurocode, with detail category $\Delta\sigma_C$ = 71 Mpa (for riveted).

The green curve is the modified fatigue strength to reflect the effects of a corrosive environment. This curve is identified as bilinear and is categorized with no fatigue limit.The curve is modified to account for the effects of a corrosive environment.

The curve has been obtained by modifying the design S-N curves of both detail category 71, given in Eurocode, and WI-rivet detail category, considered in the UK railway assessment code [1].

It can be noticed that the fatigue strength in corrosive environment, $\Delta\sigma_{D,\text{cor}}$ and $\Delta\sigma_{L,\text{cor}}$, are significantly lower that the one the one in non-corrosive environment, indicating that in corrosive environment, low stress ranges will considerably affect the fatigue life.

If $\Delta\sigma_{\text{cor}} > \Delta\sigma_{\text{D,cor}}$

$$\Delta\sigma_{\text{cor}} = \Delta\sigma_{\text{D}} \left[N_{f,\text{LCF}}^{c} \, N_{f,\text{CAFL}}^{\frac{1}{m}} \right] N_R{}^{(-c-\frac{1}{m})} \tag{4.1}$$

where $c = \dfrac{\log\left[\frac{\Delta\sigma}{\Delta\sigma_{\text{cor}}}\right]}{\log\left[\frac{N_{f,\text{CAFL}}}{N_{f,\text{LCF}}}\right]}$

If $\Delta\sigma_{\text{cor}} < \Delta\sigma_{\text{D,cor}}$

$$\Delta\sigma_{\text{cor}} = \Delta\sigma_{\text{D,cor}} \left[N_{f,\text{CAFL}}^{-\acute{c}} \right] N_R{}^{\acute{c}} \tag{4.2}$$

where $\acute{c} = \dfrac{\log\left[\frac{\Delta\sigma_{D,\text{cor}}}{\Delta L_{\text{cor}}}\right]}{\log\left[\frac{N_{f,\text{CAFL}}}{N_{f,\text{VAFL}}}\right]}$

The parameters c and $\acute{c}$ depend on the corrosion fatigue (CF) endurance of the riveted details [1].

Table 4.1: Parameters utilized in the proposed fatigue strength curve of riveted details in corrosive environments

Parameter	Eurocode Detail Category 71	
$N_{f,\text{LCF}}$	10^4	
$N_{f,\text{CAFL}}$	$5 \cdot 10^6$	
$N_{f,\text{VAFL}}$	10^8	
m, m	3 , 5	
$\Delta\sigma_{\text{C}}$ [MPa]	71	
$\Delta\sigma_{\text{D}}$ [MPa]	52.3	
$\Delta\sigma_{\text{L}}$ [MPa]	28.7	
Corrosion parameters	Urban environment	
	Mean value	Conservative value
$\Delta\sigma_{\text{D,cor}}$ [MPa]	33.5	28.0
$\Delta\sigma_{\text{L,cor}}$ [MPa]	14.9	11.5
c	0.072	0.100
$\acute{c}$	−0.271	−0.298

Table 4.1 gives the corrosion parameters based on the urban environment. It's known that marine environments tend to be more aggressive due to the presence of salt and other corrosive agents specific

to the sea. Bridges in marine environments often experience more rapid corrosion.

Nomenclature

$N_{f,\mathrm{LCF}}$	number of cycles to fatigue failure of the uncorroded materials at the yield strength
$N_{f,\mathrm{CAFL}}$	number of cycles at constant amplitude fatigue limit
$N_{f,\mathrm{VAFL}}$	number of cycles at variable amplitude fatigue limit
m	negative inverse slope of the S-N curve
c(t)	average corrosion penetration in millimetres [mm]
t	age in years
t_0	time in years of the first appearance of general corrosion
$\Delta\sigma_{\mathrm{C}}$	fatigue strength of the structural details
$\Delta\sigma_{\mathrm{D}}$	stress range at constant amplitude fatigue limit
$\Delta\sigma_{\mathrm{L}}$	stress range at variable amplitude fatigue limit
$\Delta\sigma_{\mathrm{D,cor}}$	stress range at the intersecting points of the two slopes of a corroded fatigue curve: at $N_{\mathrm{f,CAFL}}$ cycles
$\Delta\sigma_{\mathrm{L,cor}}$	stress range at $N_{\mathrm{f,VAFL}}$ cycles

4.2 Determination of corrosion wastage and effective cross-sectional parameters for corroded members

This section, is presenting how to determine the effective cross-sectional parameters, such as the cross-sectional area A_{eff} and second moment of area I_{eff}, of the corroded members.

All formulas listed listed in this section are taken from [3], by Adasooriya and Siriwardane.

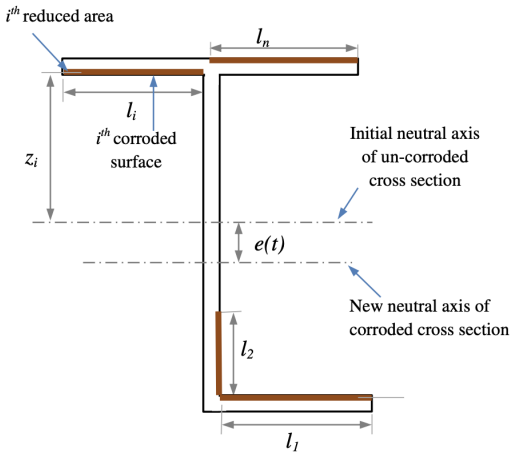

Figure 4.2: Representations of effective cross-sectional parameters of corroded (open) sections [3]

Figure 4.2 illustrate the effective cross-sectional parameters of corroded sections, considering the length and locations of the general corrosion.

4.2.1 Corrosion wastage

The cross-sectional properties are affected by the time-dependent loss of material caused by uniform corrosion, which ultimately results in a change in the overall structural stiffness during service life [1].

The corrosion wastage is presented by a nonlinear function and can be calculated with the following formula below [3]:

$$C(t) = A(t - t_0)^B;\ t > t_0 \tag{4.3}$$

where

$C(t)$ is the average corrosion penetration in millimeters (mm)

t is the age in years

t_0 is the time in years of the first appearance of general (uniform) corrosion

A and B are parameters that are determined from regression analysis of experimental data

Parameters A and B have been determined based on field tests, according to Sharifi and Paik [33].

Table 4.2: Average values for corrosion parameters A and B, for carbon [33]

Corrosive	Carbon steel	
Environment	A (mm)	B
Rural	0.0340	0.650
Urban	0.0802	0.593
Marine	0.0706	0.789

Table 4.2 displays corrosion parameters A and B for carbon steel in various environments.
It can be observed that the level of corrosion penetration is highest in urban environments, then marine environments, and the lowest in rural environments.

4.2.2 Effective cross-sectional parameters: $A_{\mathbf{eff}}(t)$ and $I_{\mathbf{eff}}(t)$

This subsection focuses on determining the effective cross-sectional area $A_{\text{eff}}(t)$ and second moment of area $I_{\text{eff}}(t)$ due to corrosion.

Uniform corrosion results in an even reduction in plate thickness, which affects the effective cross-sectional properties of the members, including effective area and second moment of area.

The effective cross-sectional area A_{eff} can be determined by the following formula:

$$A_{\text{eff}}(t) = A_0 - \sum_{i=1}^{n} C_i(t) l_i \tag{4.4}$$

where

A_0 is the initial cross-sectional area (i.e. non-corroded cross-section)

t is the age in years

$C_i(t)$ is the average corrosion penetration in milimeters (mm)

l_i is the length of general corrosion spread over the cross-section at the i^{th} corroded surface

The effective second moment of area I_{eff} can be determined according to the formula:

$$I_{\text{eff}}(t) = I_0 + A_0\, e(t)^2 - \left\{ \sum_{i=1}^{n} \left[\Delta I_i + C_i(t) l_i \left(z_i + e(t) \right)^2 \right] \right\} \tag{4.5}$$

The eccentricity $e(t)$, which represents the displacement between the new neutral axis and the initial neutral axis, can be calculated.

$$e(t) = \frac{\sum_{i=1}^{n} C_i(t)\ l_i\ z_i}{A_{\text{eff}}(t)} \tag{4.6}$$

where

z_i is the height from the initial neutral axis to the centroid of the i^{th} reduced area (i.e. lost area at the i^{th} surface)

I_0 is the initial second moment of area of the cross-section (i.e. non-corroded cross-section)

ΔI_i is the second moment of i^{th} reduced area about its own neutral axis, which is parallel to the new neutral axis of corroded cross-section

The effective cross-sectional parameters allows calculations of stresses for corroded members.

Direct stress (considering corrosion):

$$\sigma_{cor} = \frac{N}{A_{eff}} + \frac{M_{33}}{W_{el,33eff}} + \frac{M_{22}}{W_{el,22eff}} \tag{4.7}$$

$W_{el,33eff} = \frac{I_{33eff}}{zmax}$ and $W_{el,22eff} = \frac{I_{22eff}}{ymax}$ $[mm^3]$

where

$z_{\max}$, $y_{\max}$ is the distance from the new neutral axis to the furthest fiber of the corroded cross-section

4.3 Determining the fatigue life of corroded members

The number of cycles to failure N_R for corroded members can be determined by adjusting equations (4.1) and (4.2).

If $\Delta\sigma_{\text{cor}} \geq \Delta\sigma_{\text{D,cor}}$:

$$N_R = \left[\frac{\Delta\sigma_{\text{cor}}}{\Delta\sigma_{\text{D}} \cdot N_{f,\text{LCF}}^{c} \cdot N_{f,\text{CAFL}}^{\frac{1}{m}}} \right]^{\frac{1}{-c-\frac{1}{m}}} \tag{4.8}$$

If $\Delta\sigma_{\text{cor}} \leq \Delta\sigma_{\text{D,cor}}$:

$$N_R = N_{f,\text{CAFL}} \left[\frac{\Delta\sigma_{\text{cor}}}{\Delta\sigma_{\text{D,cor}}} \right]^{\frac{1}{c}} \tag{4.9}$$

where $\Delta\sigma_{\text{cor}}$ is the nominal stress range for corroded members

The damage accumulation for corroded elements, D_{cor}, can be estimated in the same way as D, using the Miner's damage rule.

$$D_{cor} = \sum_{i=1}^{n} \frac{n_i}{N_i} \quad \leq 1,0 \tag{4.10}$$

where

n_i is the number of cycles completed

N_i is the number of cycles till failure for corroded members

The fatigue life of corroded members of the bridge, can be calculated with the following formula:

$$\text{Fatigue life } = \left(\frac{1 - t_0 . D}{D_{\text{cor}}}\right) + t_0 \tag{4.11}$$

where

t_0 is the year of first of first appearance of sign of corrosion

D is the accumulated damage (per year) for an uncorroded element

D_{cor} is the accumulated damage (per year) damage for a corroded element

5 Assessment guidelines for fatigue life of existing steel bridges

A flowchart that serves as a guideline for the fatigue life assessment of existing steel bridges is proposed in this section. This guideline include the typical damage accumulation approach, from Palmgren-Miner, seen in section 3.2 and the newly proposed formula-based approach seen in section 4.1.

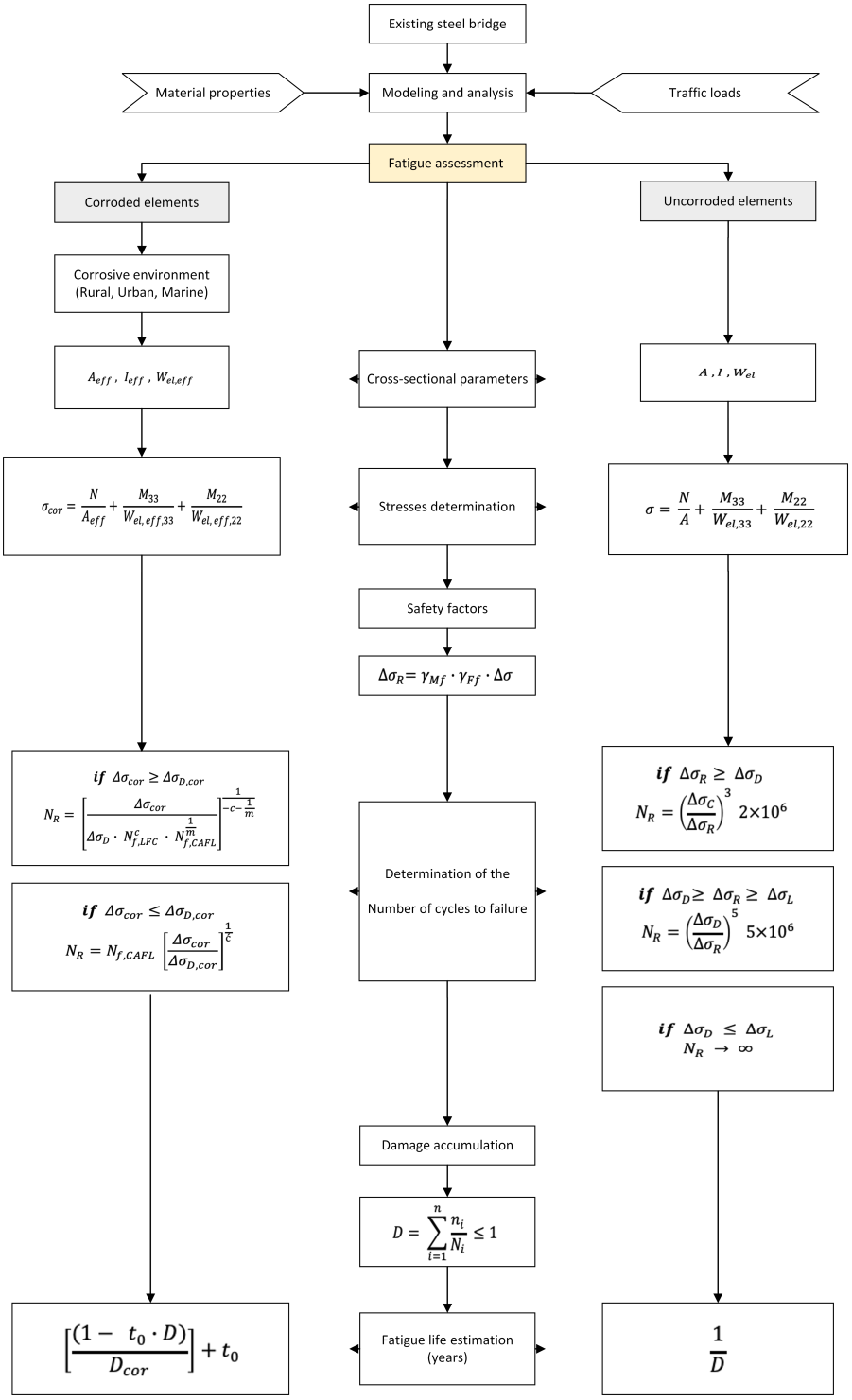

Figure 5.1: Guideline for the fatigue life assessment of existing steel bridges

This framework, figure 5.1 guide through the fatigue life estimation considering two circumstances: corrosion consideration or not.

Both scenarios have very similar steps, including the:

→ Modeling and structural analysis of the bridge

→ Determination of the cross-sectional parameters (cross-sectional area, second moment of area, section modulus)

→ Stresses and stress ranges $\Delta\sigma$ calculation

→ Fatigue safety factors (γ_{Ff} & γ_{Ff})

→ Number of cycles to failure N_R calculation

→ Calculation of the damage accumulation D

→ Fatigue life estimation

This diagram is an upgraded version of what Stave Sandviknes [34] suggested in 2021.

This framework will serve as a basis for the fatigue life analysis of the case study.

6 Case study

6.1 General description of the bridge

All the information gathered about the bridge was obtained by Bane Nor. Bane Nor is the government agency responsible for the management, maintenance, and development of the railway infrastructure in Norway.

(a) View from the track (view toward the North)

(b) View from the track (view toward the South)

(c) View from the side

Figure 6.1: Overall view of the riveted railway bridge

The studied bridge is a steel truss railway bridge built in 1906 in Norway. It crosses the river “Todøla” in the commune of Nesbyen. Trains passing through the bridge are on the Hønefoss-Bergen route, connecting the two cities. The river flows from East to West (i.e. from right to left in figure 6.1a).

The name of the bridge is "Bru over Todøla" in Norwegian, which can be translated as "Bridge above Todøla" in English.

The bridge has a total length of 25 m, a maximum height of 4 m, and a width of 4,65 m. It is a one-way bridge.

One particularity of this bridge is that it does not have wind bracing on the top chord.

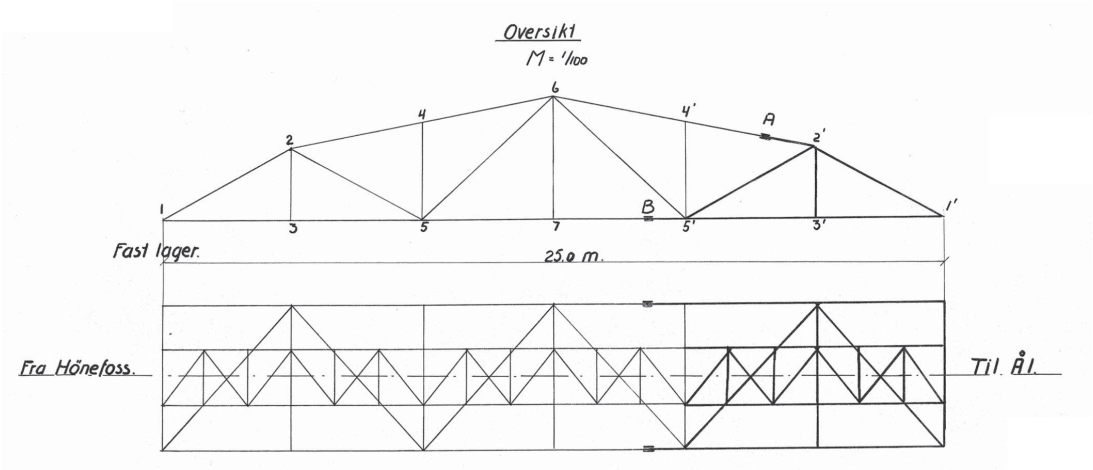

Figure 6.2: Bridge drawing - Bane Nor [35]

The darker lines in Figure 6.2 indicate the members of the bridge that were repaired in 1941, after the damage caused by the war, according to [35, p.11].

6.2 Design material properties

Th design material properties used for this case study, are the recommended values from the Eurocode and the guideline V413 from Statens Vegvesen, seen in section 2.5.

Yield strength f_y = 220
Tensile strength f_u = 350
Young's modulus E = 210 000
Shear modulus G = 81 000

6.3 Simplifications, Assumptions

General simplifications and assumptions for the calculations for this bridge are presented below.

- The design of the bridge is based on geometry from 1906 throughout the entire lifespan of the bridge. Other reconstructions/repairs are neglected.
- Figure 6.1a will be used as a reference to distinguish the right from the left. Also, to determine the positive direction of the x-axis. The trains will be considered traveling in one way only, from South to North (see compass in Figure 6.1a)
- The members on the East side are considered be on the "left side" and the members on the West side are considered to be on the "right side"
- Discontinuities due to riveted joint are neglected.

- Only GROSS sectional parameters are considered. NET cross-sectional parameters are not studied.

6.4 Cross-sections of the bridge

The Bane Nor report "KU-027964-000" [35] on fatigue calculation of the Bridge above Todøla, provides the cross-sections used in the construction of the bridge.

The bridge was constructed using built-up members that were riveted together.

Table 6.1: Cross-section descriptions and abbreviations [35]

Designations adopted in this thesis	**Designations from [35]**	**Category**	**Description**	**Location**
MG-T	OG	Main girder	Top chord truss	Main truss girder
DT	Diag	Diagonal member	Diagonal truss member	
VT	Fag	Vertical member	Vertical truss member	
MG-B	UG	Main girder	Bottom chord truss	
ST	LB	Stringer	Longitudinal beam under the rail	Bridge deck
CG	Tverr	Cross girder	Transverse beam	
CG-edge	Tverr ende	Cross girder	Transverse beam at end post	
BR	VFag 3-5-7	Bracings	Wind bracing in center	
BR-edge	VFag 1-3	Bracings	Wind bracings at end post	

The purpose of Table 6.1 is to highlight the designations (symbols) that will be assigned to each section, as well as the location of the bridge to which it corresponds.

Note: Refer to Appendix D to see the design (i.e. shape) of each cross-section.

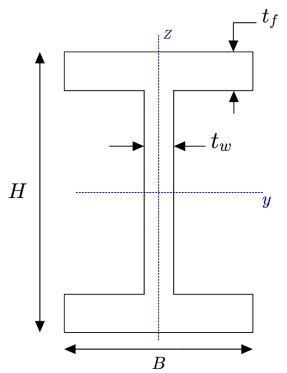

Figure 6.3: Cross-sectional axes

where

- z is the vertical axis. Defined as positive upwards.
- y is the transversal axis.
- x is the longitudinal axis, perpendicular to y- and z-axis. Positive towards the direction of train travel.

Equivalent: $I_{33} = I_y \quad I_{22} = I_z \quad W_{el,33} = W_y \quad W_z = W_{el,22}$

Table 6.2: Cross-sectional parameters, provided by SAP2000

	Center of Gravity		Area	Second Moment of Area		Section modulus	
	$z_{max}[mm]$	$y_{max}[mm]$	A $[mm^2]$	I_{33} (I_y) $[mm^4]$	I_{22} (I_z) $[mm^4]$	$W_{el,33}$ $[mm^3]$	$W_{el,22}$ $[mm^3]$
MG-T	113,8	250	16760	2,456E+08	4,943E+08	2,158E+06	1,977E+06
DT	90	220	5608	2,728E+07	1,666E+08	3,031E+05	7,574E+05
VT	85	134	8680	8,512E+06	9,264E+07	1,001E+05	6,913E+05
MG-B	150	250	11760	1,613E+08	3,902E+08	1,075E+06	1,561E+06
ST	325	105	14100	9,034E+08	1,588E+07	2,780E+06	1,512E+05
CG	485	125	21504	3,169E+09	3,475E+07	6,534E+06	2,780E+05
CG-edge	150	75	5188	7,999E+07	6,027E+06	5,333E+05	8,036E+04
BR	40,9	70	2040	7,104E+05	6,088E+06	1,737E+04	8,697E+04
BR-edge	49	90	2804	1,303E+06	1,364E+07	2,659E+04	1,516E+05

The section modulus where calculated with the corresponding formulas:

$W_{el,33} = \frac{I_{33}}{zmax}$ $[mm^3]$ and $W_{el,22} = \frac{I_{22}}{ymax}$ $[mm^3]$

6.5 Geometry and modeling in SAP2000

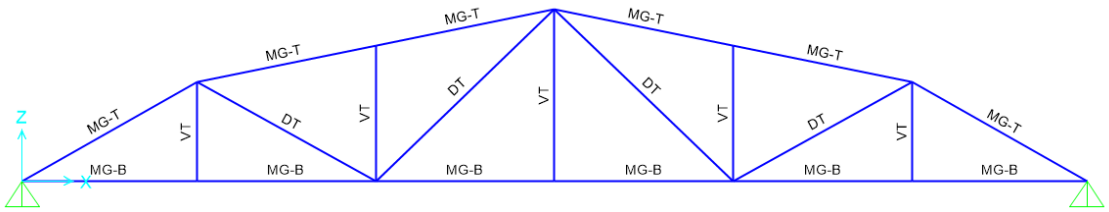

(a)

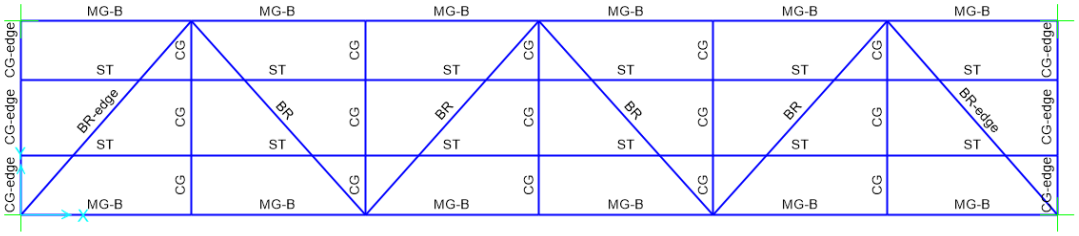

(b)

Figure 6.4: Sections of the bridge: (a) Truss girder and (b) Bridge deck

Table 6.3: Cross-sections and their corresponding numbers in SAP2000

Location	Cross-Section	Element numbering (labeling) in SAP2000	Total number of element
Truss girder	MG-T	Right side : 101, ... , 106	6
		Left side : 107, ... , 112	6
	DT	Right side: 201, ... , 204	4
		Left side: 205, ... , 208	4
	VT	Right side: 301, ... , 305	5
		Left side: 306, ... , 310	5
	MG-B	Right side: 401, ... , 406	6
		Left side: 407, ... , 412	6
Bridge deck	ST	501, ... , 512	12
	CG	601, ... , 615	15
	CG-edge	701, ... , 706	6
	BR	801, ... , 804	4
	BR-edge	901 & 902	2
			81

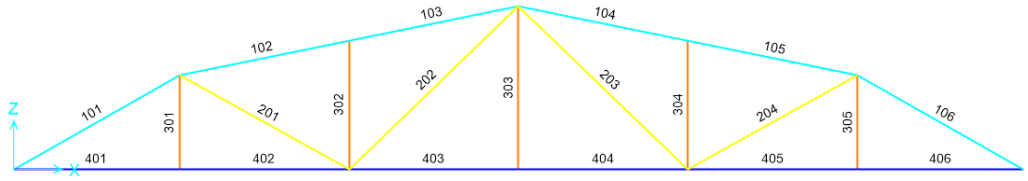

(a) Right side

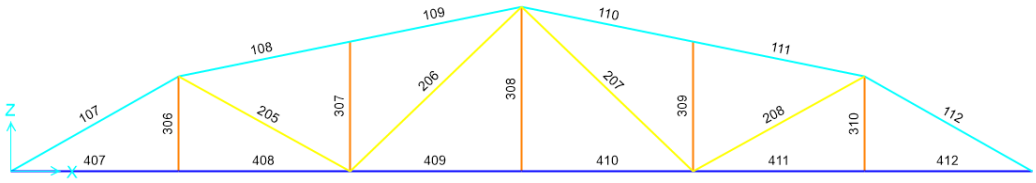

(b) Left side

Figure 6.5: Main truss girder and numbering from SAP2000

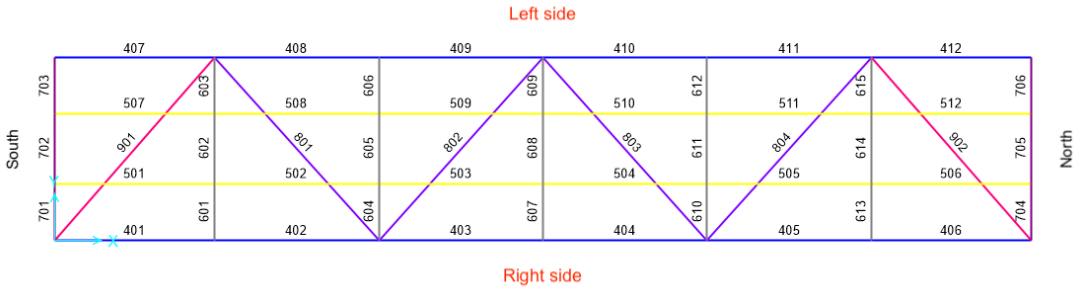

Figure 6.6: Sections numbering on the bridge deck

Note: Refer to Appendix B for more illustration of the SAP2000 model.

6.6 Corrosion on the bridge

The images below show corrosion in some members of the bridges. The images are from inspection reports from Bane Nor. Images (a) and (b) were obtained from a 2021 report [36], while images (c) and (d) were obtained from a 2015 report [37].

(a) Right side of the bridge

(b) Main truss girder

(c) Bottom chord longitudinal beam

(d) Cross-girder

Figure 6.7: Corrosion on structural members: (a) and (b) are from [36], while (c) and (d) from [37]

Based on the images Figure 6.7, corrosion will be simulated for members with following sections:

- Top chord truss (MG-T)
- Bottom chord truss (MG-B)
- Cross-girder (CG)

Assumptions for the corrosion estimation:

- Due to lack of data, it's assumed that the corrosion started after 20 years ($t_0 = 20$) for all corroded member
- The bridge is located in urban environment
- The corrosion assumed here is corrosion due to accumulation of water
- The corrosion haven't been treated since its starting
- The corrosion developed only on flanges where water accumulates
- The bridge is located in a sparsely populated area with little traffic, making the air less polluted
- There are no salt water sources in the area that can accelerate the corrosion process.

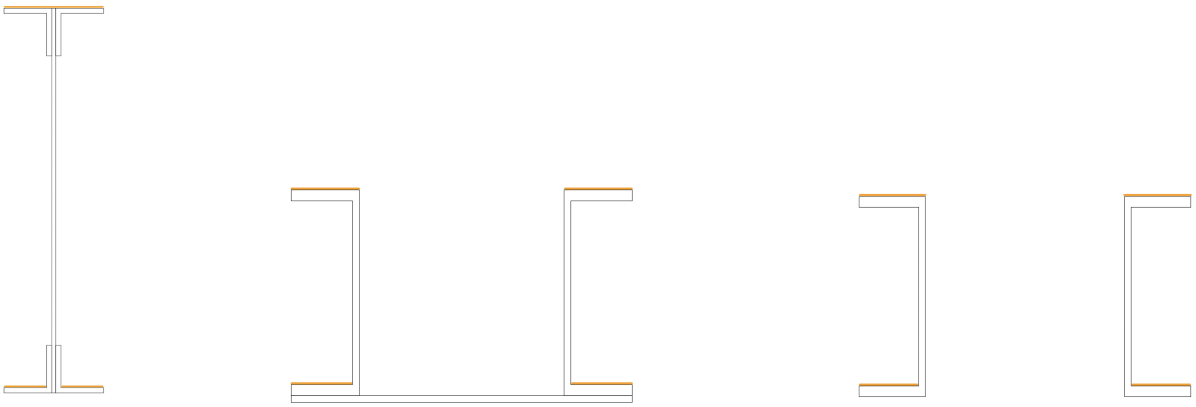

(a) Cross-girder CG *(b) Top chord MG-T* *(c) Bottom chord MG-B*

Figure 6.8: Corroded cross-sections

Figure 6.8 shows the corroded cross-sections. Each orange line represent a corroded area of thickness $C(t)$. The corrosion penetrations C(t) are calculated and illustrate in Table 6.4.

The midsection of MG-T cross-section is assumed to not have water accumulation, as from the figure 6.7b, it can be observed that the section is covered with a plate on top.

Table 6.4: Estimation of the corrosion penetration

Cross-section	Age of the member (t)	First sign of corrosion (t_0)	Average corrosion penetration C(t)
MG-T	114 years	20 years	1,2 mm
MG-B	114 years	20 years	1,2 mm
CG	114 years	20 years	1,2 mm

The average corrosion penetration has be determined using the equation 4.3.

$C(t) = A(t - t_0)^B;\ t > t_0$ in [mm]

where the corrosion parameters A = 0,0802 mm and B = 0,593 for an urban environment

Table 6.5: Cross-sectional parameters of the corroded cross-sections

	Center of Gravity		Area	Second Moment of Area		Section modulus	
	z_{max}	y_{max}	A_{eff}	$I_{33,eff}$	$I_{22,eff}$	$W_{el,33eff}$	$W_{el,22eff}$
	$[mm]$	$[mm]$	$[mm^2]$	$[mm^4]$	$[mm^4]$	$[mm^3]$	$[mm^3]$
MG-T	112,05	250	16304	2,347E+08	4,753E+08	2,094E+06	1,901E+06
MG-B	149,4	250	11304	1,520E+08	3,711E+08	1,017E+06	1,485E+06
CG	483,86	125	20947,2	3,041E+09	3,163E+07	6,286E+06	2,530E+05

The effective cross-sectional parameters in Table 6.5 were determined from AutoCAD.

7 Results

7.1 Critical fatigue life, without corrosion

The moving load analysis has revealed several critical members, with some members having a fatigue life inferior of approximately 1 year. The concerned members will be discussed in the next section 8.

The moving load analysis was performed with three different traffic mixes and the results of the most critical members are shown in the table below.

Table 7.1: Members with fatigue life inferior to 10 years

Location	Category & Designation	Members	Fatigue life (years)		
			Standard traffic mix	Light traffic mix	Heavy traffic mix
Truss girder	Bottom chord (MG-B)	401	9	19	8
		406	9	16	8
		407	9	17	7
		412	8	15	7
	Cross-girder (CG)	601	8	17	7
		603	8	17	7
		613	8	16	7
		615	8	16	7
Bridge deck	Cross-girder (CG-edge)	701 - 706	1	2	1

7.2 Reduced fatigue life considering corrosion

A total of 10 members were simulated with corrosion. The members are within the cross-section MG-T, MG-B, and CG MG-T: members 102, 103, 110 MG-B: members 403, 404, 410 CG: members 604, 606, 607, 608

The fatigue life without corrosion was performed using Palmgren-Miner damage accumulation method The fatigue life with corrosion was calculated using the proposed formulas for from the new method. The fatigue live were calculated with the three traffic mixes.

In this tables below, the results of corrosion simulation are displayed. The examination was extended to several members of a same cross-section to see how each member behave when subject to corrosion. The results have expected and unexpected values.

In light traffic mix, there is the highest reduction in fatigue life due to corrosion ; ~ 80 for some members. was supposed to be done for few members There is

Table 7.2: Case 1 - Standard traffic mix

Location	Category & Designation	Members	**Fatigue life (years)**		Reduction of fatigue life (%)
			Palmgren-Miner method *Without corrosion*	New proposed method *Considering corrosion*	
Truss girder	Top chord (MG-T)	102	90	36	61 %
		103	87	39	55 %
		111	90	39	56 %
	Bottom chord (MG-B)	403	37	25	32 %
		404	38	26	32 %
		410	31	24	23 %
Bridge deck	Cross-girder (CG)	604	29	22	22 %
		606	27	23	17 %
		607	94	35	62 %
		608	119	44	63 %

Table 7.3: Case 2 - Light traffic mix

Location	Category & Designation	Members	**Fatigue life (years)**		Reduction of fatigue life (%)
			Palmgren-Miner method *Without corrosion*	New proposed method *Considering corrosion*	fatigue life (%)
Truss girder	Top chord (MG-T)	102	269	50	82 %
		103	256	49	81 %
		111	256	50	81 %
	Bottom chord (MG-B)	403	82	31	62 %
		404	84	32	62 %
		410	67	30	55 %
Bridge deck	Cross-girder (CG)	604	55	26	52 %
		606	50	27	45 %
		607	241	42	83 %
		608	119	64	80 %

Table 7.4: Case 3 - Heavy traffic mix

Location	Category & Designation	Members	**Fatigue life (years)**		Reduction of fatigue life (%)
			Palmgren-Miner method *Without corrosion*	New proposed method *Considering corrosion*	
Truss girder	Top chord (MG-T)	102	82	38	54 %
		103	79	37	53 %
		111	83	38	54 %
	Bottom chord (MG-B)	403	35	25	28 %
		404	33	25	25 %
		410	28	23	18 %
Bridge deck	Cross-girder (CG)	604	26	22	15 %
		606	25	22	12 %
		607	87	39	55 %
		608	107	43	59 %

8 Discussion

This discussion section will interprete the obtained results and try to explained any deviations or unexpected values.

8.1 Extreme fatigue life without considering corrosion

The bridge doesn't satisfy the Eurocode requirement for fatigue design, neither for "standard traffic mix", "light traffic mix" or "heavy traffic mix". Several members are failing in less than 50 years. Appendix C lists all members failing before 50 years of life service.

Some members have been noticed with a fatigue life ~ 1 year,

8.1.1 Cross-girder members (CG-edge)

Members 701-706, corresponding to the cross-girder at both end (longitudinal) of the bridge are observed with a low fatigue life, about 1-3 years. This is the lowest fatigue life of all members in the bridge. These members correspond to the cross-girders CG-edge.

Hypothesis 1 (H1):

Members 701-706 failed due to their low cross-sectional parameters (area and section modulus).
Evaluation (H1): A cross-section with higher parameters, CG, has been replaced the section CG-egde
Results (H1): The fatigue life of members 701-706 have remained the same, even with higher cross-sectional characteristics element. Another thing observed was that, the fatigue life of other members were improved, except for 701-706 members.

Hypothesis 2:

This problem is be due to the thesis bridge modeling in SAP2000 (even though the model has been checked several times).

Hypothesis 3:

The issue is due to the overall design/conception of the original bridge, and how the way the members are redistributing the loads between them.

According to Parodi-Figueroa et al. [38], the Sustainable Bridges European project [39] indicated that, for historic open deck riveted truss bridges, fatigue problems usually start in the transverse structure since these short elements have to endure more stress cycles than the main girder's components.

Parodi-Figueroa et al. [38], are also stating that "stringer-to-floor-beams" connections on historic riveted

railway bridges were identified as the components most prone to fatigue failure. They mean by that, that the connections between stringers and cross-girder are the weakest to resist fatigue.

8.2 Reduced fatigue life due to corrosion

This is the main focus of this thesis, i.e., look at how the corrosion affect the fatigue life the bridge. As the study was performed with three different traffic mixes, each one will be examined individually, and then the entire group will be analyzed together to define a pattern.

As seen in previous Tables 7.2, 7.3, and 7.4, the fatigue life is reduce when corrosion is applied

The corrosion simulations of sections of the bridge was performed to several members to examinate the applicability of the proposed formula for corroded members.

8.2.1 Individual observations

One of the first remarks noticed during the fatigue calculation of corroded members is that, members with a fatigue life (without corrosion) inferior to t_0 (20 years) were failing before corrosion is applied. So there were no necessity take them into account for corrosion simulation.

Top truss MG-T:

The studied members 102, 103, and 111 show a reduction in fatigue life of 55-61 % in standard traffic mix, 81-82 % with light traffic mix, and 53-54 % within heavy traffic mix.

Bottom truss MG-B:

The studied members 403, 404, and 410 are displaying a reduction of fatigue life of 23-32 % with a standard traffic mix, 55-62 % with a light traffic mix, and 18-28 % within a heavy traffic mix.

Cross-girder CG:

It can be observed the members 604 and 605 are losing 17-22 % of fatigue life in standard traffic mix, 45-52 % of fatigue life in light traffic mix, and 12-15 % of fatigue life in heavy traffic mix

Members 607 and 608 are losing 62-63 % of fatigue life in standard traffic mix, 80-83 % of fatigue life in light traffic mix, and 55-59 % of fatigue life in heavy traffic mix.

Two conclusion and observation can be made from that. One is that the effect of corrosion doesn't affect linearly all cross-girder members. Its seems that the location of the member has an influence. The other observation is that the fatigue life if more affected in case of light traffic mix.

One more note is that, without corrosion, members 607 and 608 have a significantly high fatigue life than members 604 and 605. However, considering corrosion, members 607 and 608 are loosing a higher

percentage of their fatigue life.

8.2.2 Global observations

One of the general observation than can be made of the individual observations is that, in light traffic, the fatigue life reduction is the highest considering all members. In second position is the standard traffic mix.

The significant reduction in fatigue life, up to approximately 80 %, was unexpected.

8.3 Differences between the two methods for fatigue life assessment

Although Miner's approach is widely used and it is applicable to any type of bridge and any details category, the newly proposed formula represent few advantages.
It can directly apply to any steel or wrought iron riveted structural details, without requiring additional CF tests or any corrosive parameters It takes directly into account the effect of the corrosive environment on the bridge and can be applied to urban or marine environment.

8.4 Reliability of the results and reflection on the results

In carrying out this project, errors and mistakes are not to be excluded. The modelling of the bridge and the analysis were carried out with the data available. The calculations of fatigue lives with and without corrosion were calculated according to the methods presented above, and summarized in Section 5. The results obtained were satisfactory as they confirmed the general idea of reduced fatigue life due to corrosion. However, some reductions in fatigue life have been observed extremely high. This could be correct, a fatigue loss of 80 % due to corrosion, but errors, about the calculations, are not to be excluded.

One of the main challenges in this project was to work with three different traffic mixes, knowing that the bridge respond differently to each traffic mix.

9 Conclusion

9.1 Conclusion and Summary

Although it was not the main focus of the thesis, several members were observed to not meet the Eurocode requirements about fatigue. The bridge has been tested with three of the traffic mixes, and several members have been noticed with a fatigue life inferior to 10 years, and many other with a fatigue life inferior to 50 years. The most critical one are the cross-girder member 701-706, with a fatigue life of approximately 1 year.

As declared Biezma and Schanack [10, p. 400], in the 19^{th} century, before design standards existed, engineers underestimated the load of the new railway traffic.

An explanation for the early failure of these members is based on certain assumptions: members and bridge geometry remained unchanged from their original design.

Parodi-Figueroa et al. [38] also highlight that, for historic open deck riveted truss bridges, fatigue problems usually start in the transverse structure since these short elements have to endure more stress cycles than the main girder's components.

The main objective of this thesis was to calculate the fatigue life of the bridge's corroded members using a newly proposed method, and to compare these results with those from the conventional Miner's rule to evaluate its applicability and significance.

An assessment guideline that lead through the different steps for the estimation of the fatigue life of existing steel bridges was established in section 5.

A total of 10 members were simulated with corrosion, including: three members (102, 103, and 111) from top chord truss MG-T, three members (403, 404, and 410) from bottom chord truss MG-B, and four members (604, 605, 607, and 608) from cross-girder CG.

The study has revealed a reduction of fatigue life within the range of 12-83 %. As expected, the fatigue life of corroded members were lower compared to those without corrosion.

Standard traffic mix:
MG-T members (102, 103, and 111) have lost 55-61 % of their fatigue life. MG-B members (403, 404, and 410) have lost 23-32 %. CG members (604 and 605) have lost 17-22 %. CG members (607 and 608) lost 62-63 %.

Light traffic mix:
MG-T members (102, 103, and 111) have lost 81-82 % of their fatigue life. MG-B members (403, 404,

and 410) have lost 55-62 %. CG members (604 and 605) have lost 45-52 %. CG members (607 and 608) lost 80-83 %.

Heavy traffic mix:
MG-T members (102, 103, and 111) have lost 53-54 % of their fatigue life. MG-B members (403, 404, and 410) have lost 18-28 %. CG members (604 and 605) have lost 12-15 %. CG members (607 and 608) lost 55-59 %.

Several observations have been observed:

- the reduction of fatigue life is the highest with a light traffic mix
- CG members (604 and 605) react differently to the same corrosion compared CG members (607 and 608).
- MG-T members and CG members (607 and 608) are loosing up to 80 % of their live in light traffic mix.
- CG members (604 and 605) have always the lowest reduction of life, in all traffic mixes

A list of factors that influence the reduction fatigue life (%) was made from these observations, including:

→ type of traffic loading (i.e. traffic mixes)

→ cross-sectional parameters (area A, second moment of area I, section modulus $W_{,el}$)

→ the type of cross-sections

→ the locations of the members

Other points will need to be addressed in future work, such as why a "light traffic mix" resulted in a greater reduction in fatigue life. One theory is that light traffic results in more cycles per day or per year.

It can be concluded that the new method from Adasooriya et al. provides a more accurate and reliable assessment of the fatigue life of existing bridges. This method accounts for additional factors, such as material loss and reduced fatigue strength (S-N curve) due to corrosion over time.

As noted in the literature review, bridges can collapse unexpectedly, sometimes without warning. Therefore, it is crucial to consider all factors that can degrade a bridge's fatigue life, including environmental conditions.

9.2 Further work

To go further, several work can be performed.

The analysis of the time-dependent change of mechanical properties on fatigue life, combined to corrosion.
As discovered Moi [25], the material properties for old bridges might be lower than the recommended values from the Eurocodes.

Adasooriya and Siriwardane [3] highlight that the time-dependent change of cross-sectional shapes due to loss of material caused by the general corrosion and related change of rigidities (i.e. change of axial, bending, torsional and warping rigidities) may cause a change of the overall stiffness of the structure and structural behaviour (i.e. stress, displacement and dynamic properties).

Another further work, for more reliable life estimation, will depend on available data about the bridge.

Actual traffic: fatigue life estimation based on actual traffic load will provide more reliable results

Corrosion data: as seen in the case study section, a lot of assumptions were made to perform this study. In real life, the corrosion locations and thickness is different on every member.

Replaced elements: The new incorporated members and the actual design in important to know how the bridge behave under fatigue loading.

Net cross-sectional parameters: The "net" cross-sectional parameters are the one that need to be taken into account for the fatigue life estimation. As the members are drilled for the the riveting, the cross-sectional parameters and the also are affected.

Stress concentrations: Due to the wholes made into the cross sections, stresses might concentrate in those areas and cracks might start.

References

[1] N. Adasooriya, T. Hemmingsen, and D. Pavlou, "S-n curve for riveted details in corrosive environment and its application to a bridge," Fatigue & Fracture of Engineering Materials & Structures, vol. 43, no. 6, pp. 1199–1213, 2019, ISSN: 8756-758X, 1460-2695. DOI: 10.1111/ffe.13193. [Online]. Available: https://onlinelibrary.wiley.com/doi/10.1111/ffe.13193.

[2] B. M. Imam and T. D. Righiniotis, "Fatigue evaluation of riveted railway bridges through global and local analysis," Journal of Constructional Steel Research, vol. 66, no. 11, pp. 1411–1421, Nov. 1, 2010, ISSN: 0143-974X. DOI: 10.1016/j.jcsr.2010.04.015. [Online]. Available: https://www.sciencedirect.com/science/article/pii/S0143974X10001355.

[3] N. D. Adasooriya and S. C. Siriwardane, "Remaining fatigue life estimation of corroded bridge members," Fatigue & Fracture of Engineering Materials & Structures, vol. 37, no. 6, pp. 603–622, Jun. 2014, ISSN: 8756-758X, 1460-2695. DOI: 10.1111/ffe.12144. [Online]. Available: https://onlinelibrary.wiley.com/doi/10.1111/ffe.12144.

[4] N. D. Adasooriya, T. Hemmingsen, and D. Pavlou, "Environment-assisted corrosion damage of steel bridges: A conceptual framework for structural integrity," Corrosion Reviews, vol. 38, no. 1, pp. 49–65, 2019, ISSN: 2191-0316, 0334-6005. DOI: 10.1515/corrrev-2019-0066. [Online]. Available: https://www.degruyter.com/document/doi/10.1515/corrrev-2019-0066/html.

[5] B. Kühn, M. Luki, S. Walbridge, B. Androic, O. Dijkstra, and Ö. Bucak, "Assessment of existing steel structures: Recommendations for estimation of remaining fatigue life," 2008.

[6] T. Siwowski, "Fatigue assessment of existing riveted truss bridges: Case study," Bulletin of the Polish Academy of Sciences Technical Sciences, vol. 63, no. 1, pp. 125–133, Mar. 1, 2015, ISSN: 2300-1917. DOI: 10.1515/bpasts-2015-0014. [Online]. Available: http://journals.pan.pl/dlibra/publication/97521/edition/84109/content.

[7] M. Rajchel and T. Siwowski, "Fatigue assessment of a 100-year-old riveted truss railway bridge," Journal of Constructional Steel Research, vol. 217, p. 108 662, Jun. 2024, ISSN: 0143974X. DOI: 10.1016/j.jcsr.2024.108662. [Online]. Available: https://linkinghub.elsevier.com/retrieve/pii/S0143974X24002128.

[8] M. N. James, "Fracture-safe and fatigue-reliable structures," Frattura ed Integrità Strutturale, vol. 8, no. 30, pp. 293–303, Sep. 8, 2014, Number: 30, ISSN: 1971-8993. DOI: 10.3221/IGF-ESIS.30.36. [Online]. Available: https://www.fracturae.com/index.php/fis/article/view/1276.

[9] N. Subramanian, "I-35w mississippi river bridge failure – is it a wake up call?,"

[10] M. V. Biezma and F. Schanack, "Collapse of steel bridges," Journal of Performance of Constructed Facilities, vol. 21, no. 5, pp. 398–405, Oct. 2007, ISSN: 0887-3828, 1943-5509. DOI: 10.1061/(ASCE)0887-3828(2007)21:5(398). [Online]. Available: https://ascelibrary.org/doi/10.1061/%28ASCE%290887-3828%282007%2921%3A5%28398%29 (visited on 06/14/2024).

[11] T. Larsson, "Material and fatigue properties of old metal bridges," 2006, Publisher: Luleå tekniska universitet. [Online]. Available: https://urn.kb.se/resolve?urn=urn:nbn:se:ltu:diva-26503.

[12] T. Larsson, "Fatigue assessment of riveted bridges," Ph.D. dissertation, Luleå University of Technology, Sweden, 2009.

[13] H. Jakubczak, W. Sobczykiewicz, and G. Glinka, "Fatigue reliability of structural components," International Journal oF Materials & Product Technology, vol. 25, pp. 64–83, Jan. 1, 2006. DOI: 10.1504/IJMPT.2006.008274.

[14] R. W. Revie and H. H. Uhlig, Corrosion and Corrosion Control : An Introduction to Corrosion Science and Engineering.

[15] J. M. Kulicki and National Research Council (U.S.), Eds., Guidelines for evaluating corrosion effects in existing steel bridges, National cooperative highway research program report 333, Washington, D.C: Transportation Research Board, National Research Council, 1990, 140 pp., ISBN: 978-0-309-04856-9.

[16] M. Tavakkolizadeh and H. Saadatmanesh, "Galvanic corrosion of carbon and steel in aggressive environments," Journal of Composites for Construction, vol. 5, no. 3, pp. 200–210, Aug. 2001, ISSN: 1090-0268, 1943-5614. DOI: 10.1061/(ASCE)1090-0268(2001)5:3(200). [Online]. Available: https://ascelibrary.org/doi/10.1061/%28ASCE%291090-0268%282001%295%3A3%28200%29.

[17] M. T. Gebremeskel and A. T. Cruz, "Fatigue life assessment of a steel bridge based on measured corrosion wastage and actual traffic loading," Department: Mechanical and Structural Engineering and Materials science, Master's thesis, University of Stavanger, Stavanger, 2022.

[18] D. A. Bayliss and D. H. Deacon, "Steelwork corrosion control," 2002.

[19] J. R. Kayser, "The effects of corrosion on the reliability of steel girder bridges.," Accepted: 2020-09-09T03:01:25Z, Thesis, 1988. [Online]. Available: http://deepblue.lib.umich.edu/handle/2027.42/161817.

[20] R. Landolfo, C. Lucrezia, and F. Portioli, "Modeling of metal structure corrosion damage: A state of the art report," Sustainability, vol. 2, Jul. 1, 2010. DOI: 10.3390/su2072163.

[21] J. Kruger, "Cost of metallic corrosion," in Uhlig's Corrosion Handbook, R. W. Revie, Ed., 1st ed., Wiley, Mar. 28, 2011, pp. 15–20, ISBN: 978-0-470-08032-0 978-0-470-87286-4. DOI: 10.1002/

9780470872864 . ch2. [Online]. Available: https : / / onlinelibrary . wiley . com / doi / 10 . 1002 / 9780470872864.ch2.

[22] "World bank open data," World Bank Open Data. (), [Online]. Available: https://data.worldbank.org (visited on 06/04/2024).

[23] J. Choudhury and A. Hasnat, Bridge collapses around the world: Causes and mechanisms. Aug. 21, 2015.

[24] R. N. Clark, R. Burrows, R. Patel, S. Moore, K. R. Hallam, and P. E. J. Flewitt, "Nanometre to micrometre length-scale techniques for characterising environmentally-assisted cracking: An appraisal," Heliyon, vol. 6, no. 3, e03448, Mar. 1, 2020, ISSN: 2405-8440. DOI: 10 . 1016 / j . heliyon . 2020 . e03448. [Online]. Available: https : / / www . sciencedirect . com / science / article / pii/S2405844020302930.

[25] P. K. Moi, "Integrity assessment of mechanical properties and microstructure in aging railway bridge in norway," Department: Mechanical and Structural Engineering and Materials science, Master's thesis, University of Stavanger, Stavanger, 2023.

[26] V412: Bæreevneklassifisering av bruer, laster, 2023. [Online]. Available: https : / / viewers . vegnorm . vegvesen . no / product / 859962 ? langUI = nb & filePath = 536b7c87 - 4115 - 4843 - 93e4 - d0572de84af0.pdf&fileType=Pdf.

[27] V413 bæreevneklassifisering av bruer, materialer, 2023. [Online]. Available: https : / / viewers . vegnorm.vegvesen.no/product/859963/nb.

[28] EN 1993-1-1 (2005): Eurocode 3: Design of steel structures - part 1-1: General rules and rules for buildings.

[29] NS-EN 1993-2:2006+NA:2009. eurocode 3: Design of steel structures - part 2: Steel bridges.

[30] M. Al-Emrani and M. Aygül, "Fatigue design of steel and composite bridges," 2014, ISSN: 1652-9162.

[31] BS EN 1993-1-9:2005. eurocode 3: Design of steel structures - part 1-9: Fatigue.

[32] NS-EN 1991-2:2003+NA:2010. eurocode 1: Actions on structures - part 2: Traffic loads on bridges.

[33] Y. Sharifi and J. K. Paik, "Ultimate strength reliability analysis of corroded steel-box girder bridges," Thin-Walled Structures, vol. 49, no. 1, pp. 157–166, Jan. 2011, ISSN: 02638231. DOI: 10.1016/j.tws.2010.09.001. [Online]. Available: https://linkinghub.elsevier.com/retrieve/pii/S0263823110001576.

[34] J. S. Stave Sandviknes, "Environment-assisted fatigue of steel bridges: A conceptual framework for structural integrity/life assessment," Department: Mechanical and Structural Engineering and Materials science, Master's thesis, University of Stavanger, Stavanger, 2021.

[35] "Beregningsrapport - utmattingsberegninger av eldre jernbanebruer: Bru over todøla," Bane Nor, Norway, Technical Report KU-027964-000, 2018.

[36] “Brurapport,” Bane Nor, Norway, Technical Report KU-BRU-002906, 2021.

[37] “Hovedinspeksjon av bruer bergensbanen: Bru over todøla,” Bane Nor, Norway, Technical Report KU-015745-000, 2015.

[38] C. Parodi-Figueroa, D. D’Ayala, and W. Sebastian, “Fatigue assessment of historic retrofitted through-truss riveted railway bridge,” Engineering Structures, vol. 307, p. 117 812, May 15, 2024, ISSN: 0141-0296. DOI: 10.1016/j.engstruct.2024.117812. [Online]. Available: https://www.sciencedirect.com/science/article/pii/S0141029624003742.

[39] J. S. Jensen, J. R. Casas, R. Karoumi, M. Plos, C. Cremona, and C. Melbourne, “Guideline for load and resistance assessment of existing european railway bridges,” in Fourth International Conference on Bridge Maintenance, Safety and Management (IABMAS 08), France, Jul. 2008, pp 3658–3665. [Online]. Available: https://hal.science/hal-00400382.

A Appendix: Bridge drawing

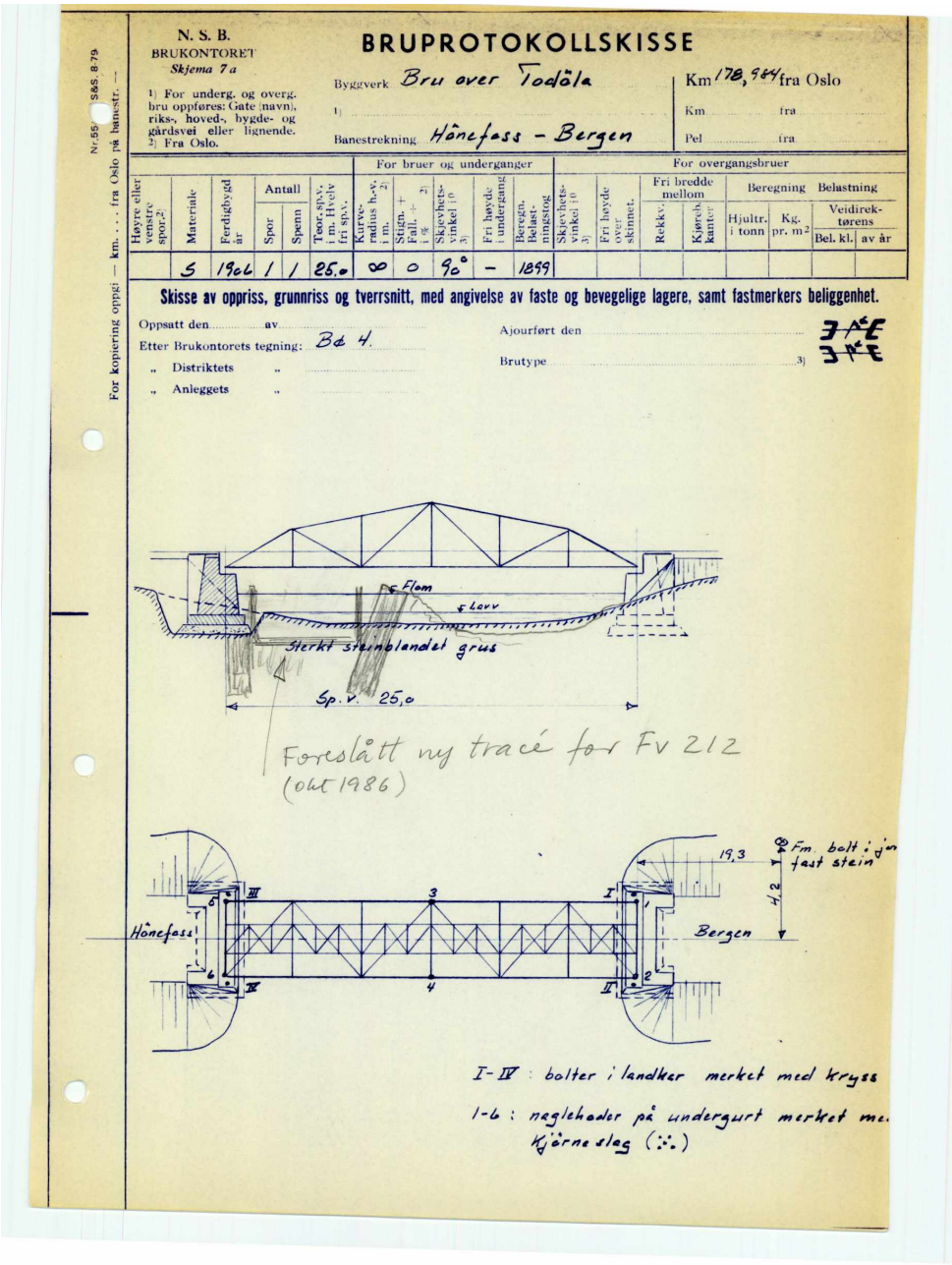

Figure A.1: Bridge drawing

B Appendix: Additional illustrations of the bridge modeling

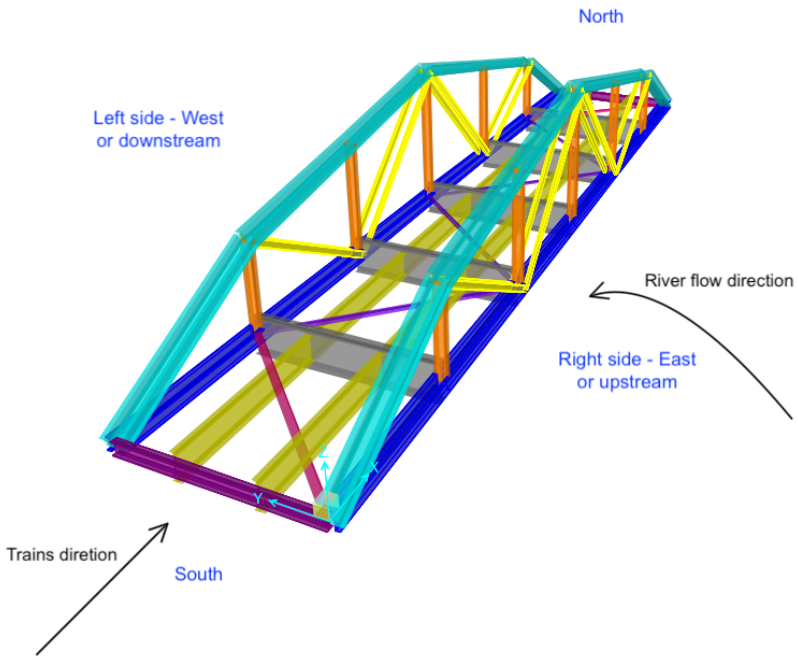

Figure B.1: 3D modeling of the bridge

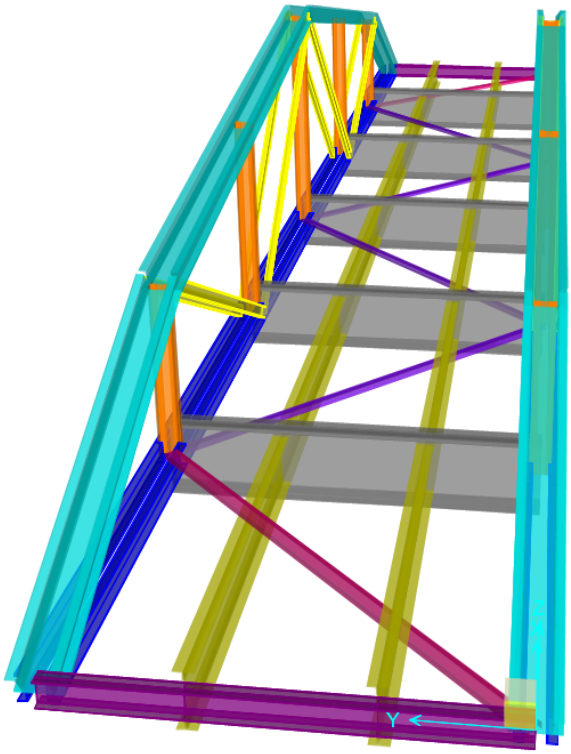

Figure B.2: 3D modeling of the bridge

C Appendix: Fatigue life inferior to 50 years, of members of the bridge

Table C.1: Fatigue life, < 50 years, of members from the main truss girder

Category & Designation	Members	**Fatigue life (years)**		
		Standard traffic mix	Light traffic mix	Heavy traffic mix
Top chord truss (MG-T)	101	14	27	11
	106	13	23	11
	107	14	27	11
	112	13	23	11
Cross-girder (CG)	201	23	35	21
	202	45	68	38
	203	44	66	39
	204	28	35	25
	205	26	39	22
	206	44	68	38
	207	44	66	38
	208	32	40	27
Vertical truss (VT)	301	28	49	21
	305	23	37	19
	306	29	53	23
	310	26	42	21
Bottom chord truss (MG-B)	401	9	19	8
	402	19	41	17
	403	37	82	35
	404	38	84	33
	405	21	41	17
	406	9	16	8
	407	9	17	7
	408	25	57	22
	409	30	66	28
	410	31	67	28
	411	25	53	23
	412	8	15	7

Table C.2: Fatigue life, < 50 years, of members from the bridge deck

Category & Designation	Members	**Fatigue life (years)**		
		Standard traffic mix	Light traffic mix	Heavy traffic mix
Stringer (ST)	501	19	37	16
	502	16	27	13
	505	14	24	12
	506	17	29	15
	507	14	26	12
	508	19	31	17
	511	18	28	14
	512	12	21	11
Cross-girder (CG)	601	8	17	7
	602	21	43	18
	603	8	17	7
	604	29	55	26
	606	27	50	25
	610	30	57	26
	612	29	51	25
	613	8	16	7
	614	19	40	16
	615	8	16	7
Cross-girder (CG-edge)	701	1	1	1
	702	1	3	1
	703	1	1	1
	704	1	1	1
	705	1	2	1
	706	1	1	0

Finally, there is 53 members in a total of 81 members, with one fatigue life under 50 years depending on the traffic mix.

D Appendix: Cross-sections of the bridge

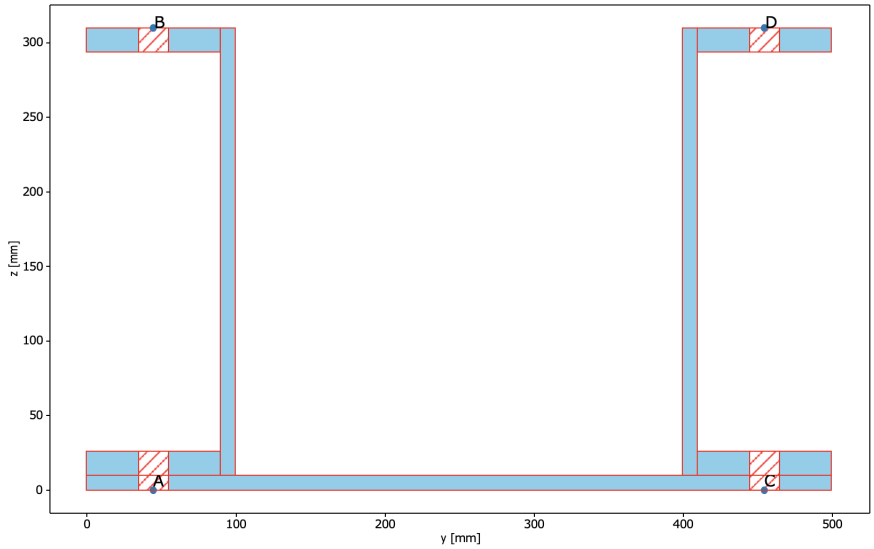

Figure D.1: Main girder - Top chord (MG-T)

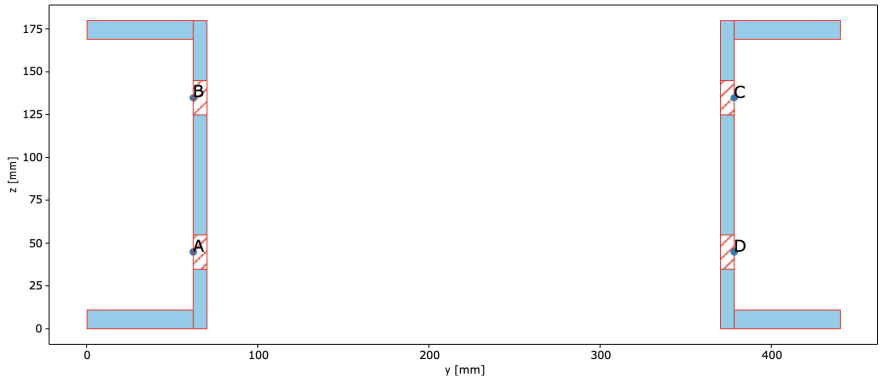

Figure D.2: Diagonal truss member (DT)

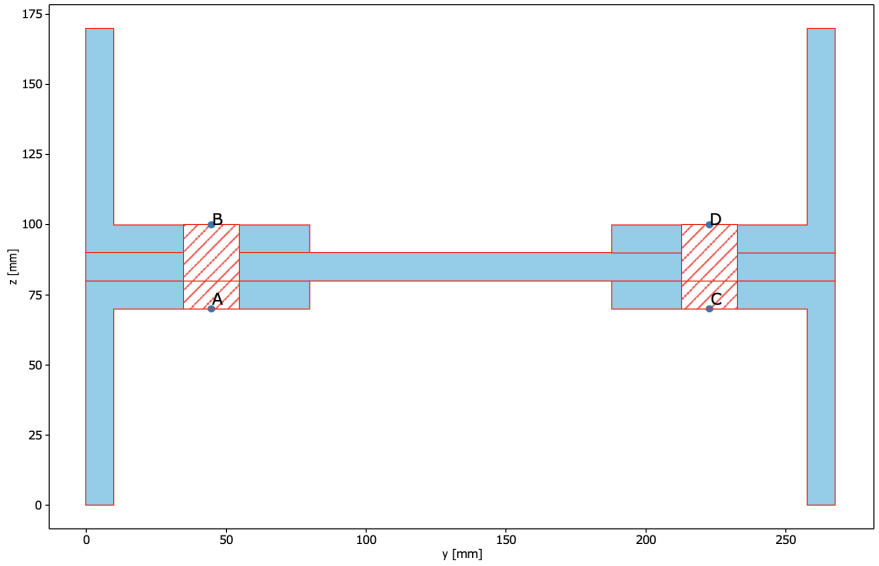

Figure D.3: Vertical truss member (VT)

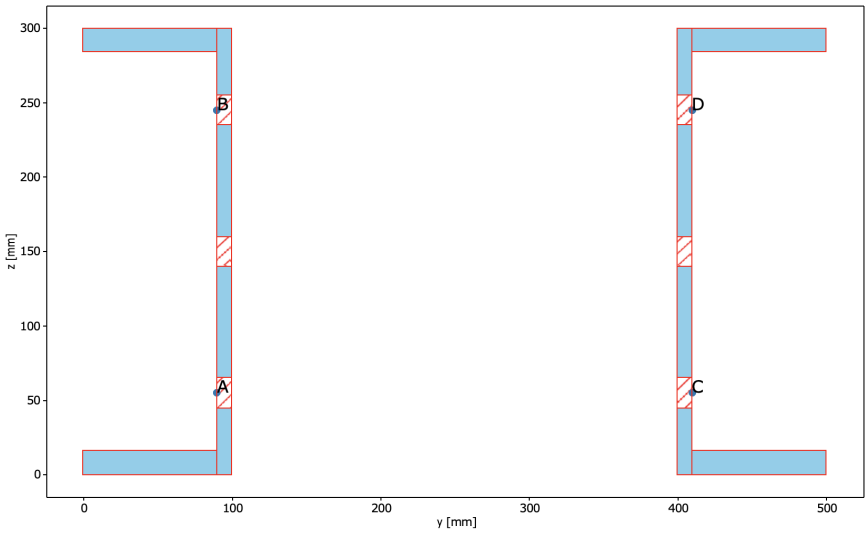

Figure D.4: Main girder - Bottom chord (MG-B)

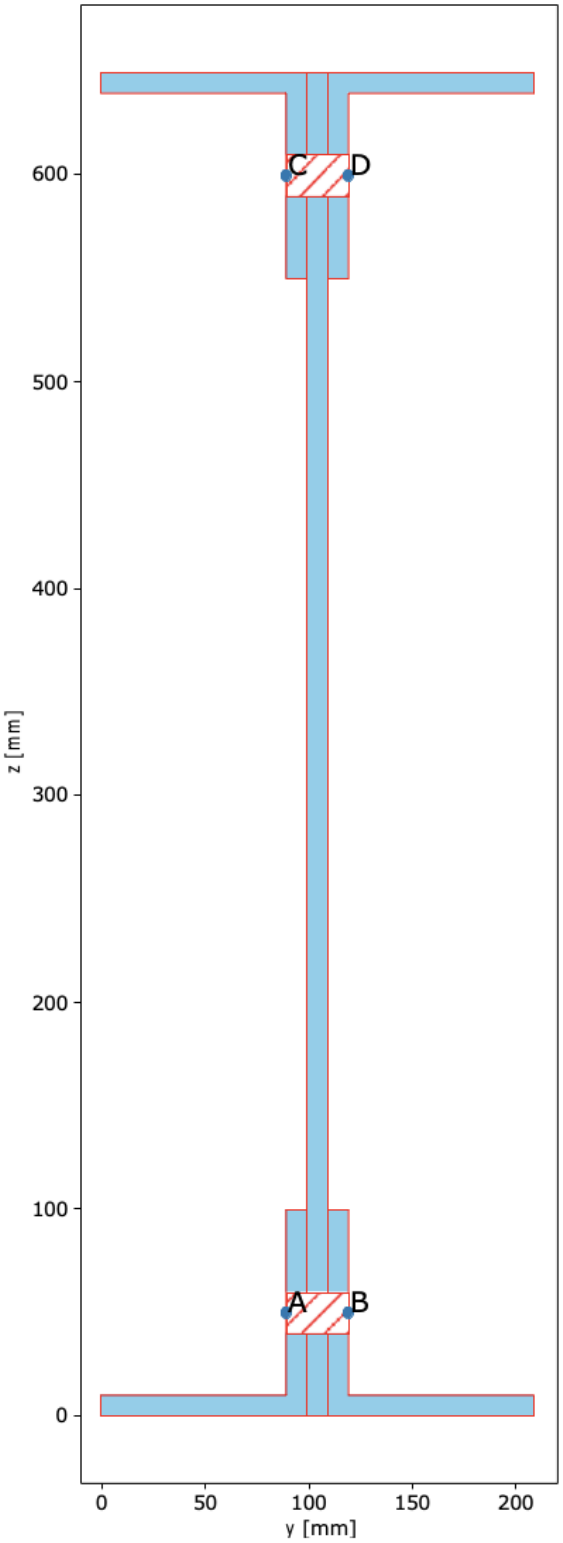

Figure D.5: Stringer (ST)

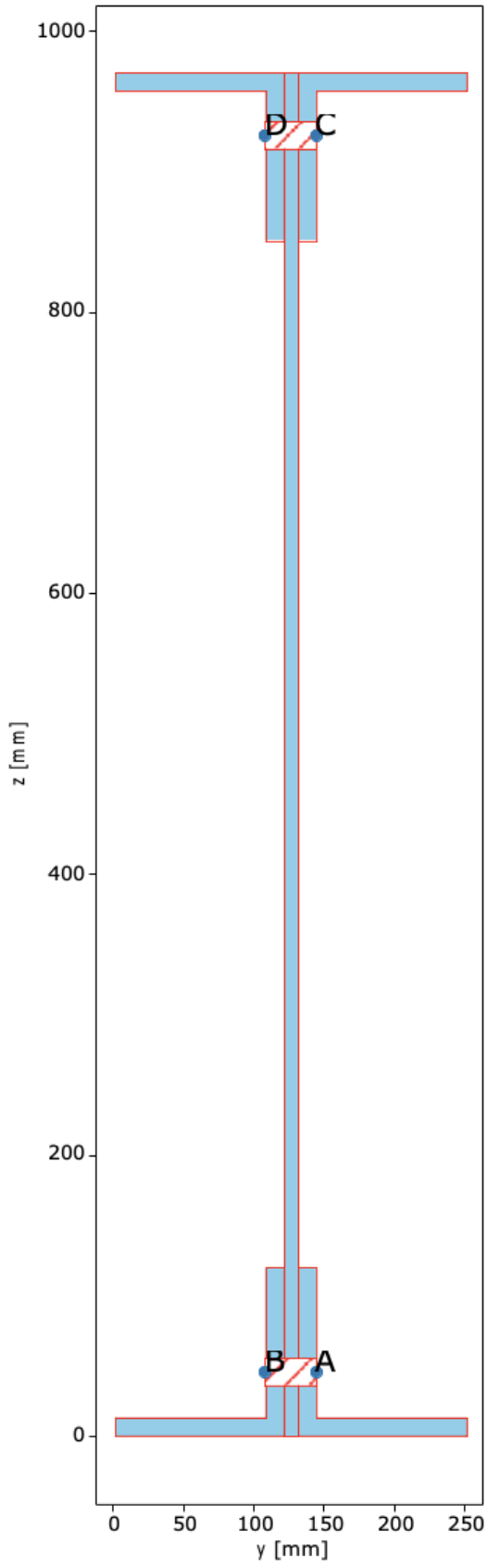

Figure D.6: Cross girder (CG)

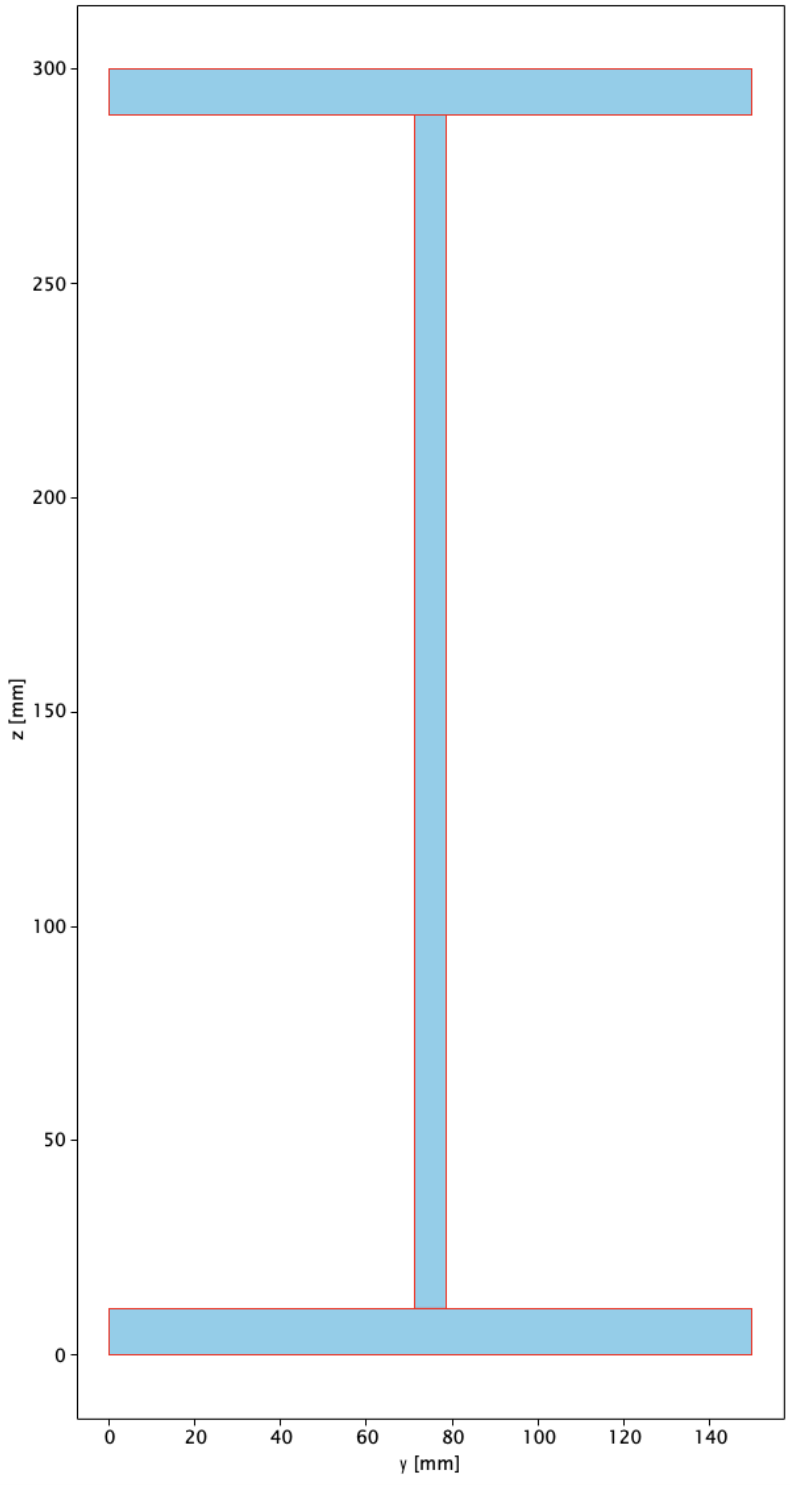

Figure D.7: Cross girder (CG-edge)

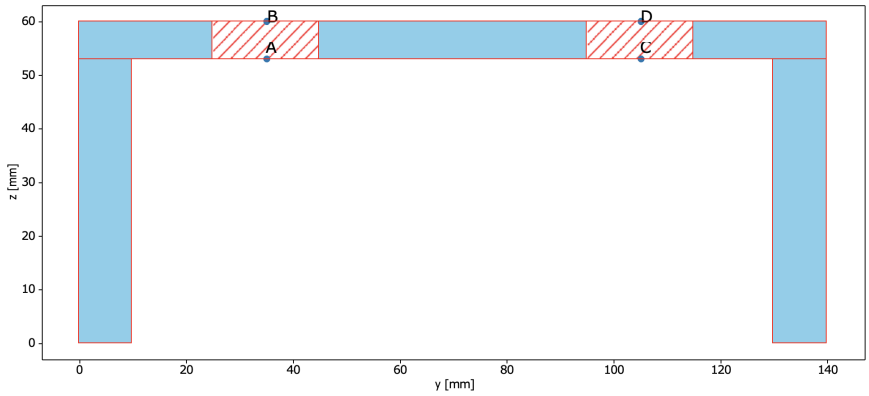

Figure D.8: Wind bracing (BR)

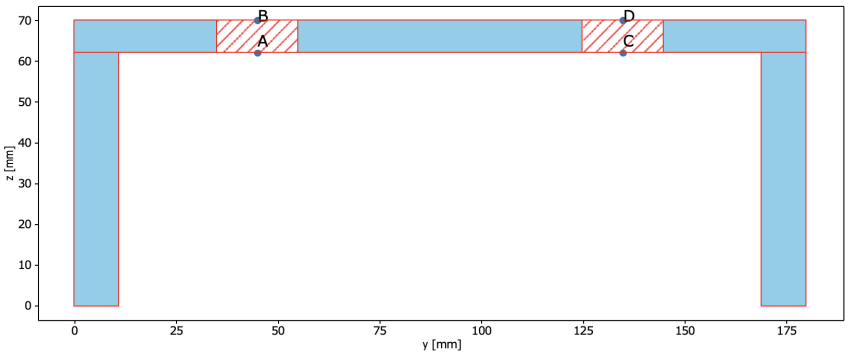

Figure D.9: Wind bracing (BR-edge)

Table D.1: Cross-section dimensions

Cross-section	**Detail**	**Length (L)** [mm]	**Thickness (t)** [mm]
MG-T	Webs (vertical)	300	10
	Flanges	90	16
	Bottom horizontal plate	500	10
DT	Web	180	8
	Flanges	62	11
	Back to back distance	300	
VT	Web	268	10
	L-profil	80	10
MG-B	Web	300	10
	Flanges	90	16
	Back to back distance	300	
ST	Web	650	10
	L-profil	100	10
CG	Web	970	10
	L-profil	120	13
CG-edge	Web	278,6	7,1
	Flanges (total length)	150	10,7
BR	Web	140	7
	Flanges	53	10
BR-edge	Web	180	8
	Flanges	62	11

E Appendix: Train types used for railway bridges fatigue assessment [EN 1991-2]

Type 1 Locomotive-hauled passenger train

$\Sigma Q = 6630\text{kN}$ $V = 200\text{km/h}$ $L = 262{,}10\text{m}$ $q = 25{,}3\text{kN/m'}$

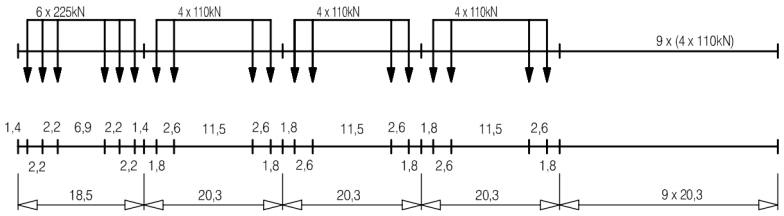

Figure E.1: Train type 1

Type 2 Locomotive-hauled passenger train

$\Sigma Q = 5300\text{kN}$ $V = 160\text{km/h}$ $L = 281{,}10\text{m}$ $q = 18{,}9\text{kN/m'}$

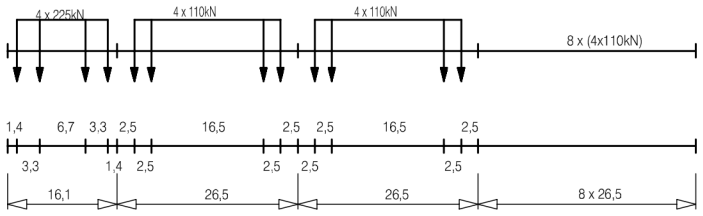

Figure E.2: Train type 2

Type 3 High speed passenger train

$\Sigma Q = 9400\text{kN}$ $V = 250\text{km/h}$ $L = 385{,}52\text{m}$ $q = 24{,}4\text{kN/m'}$

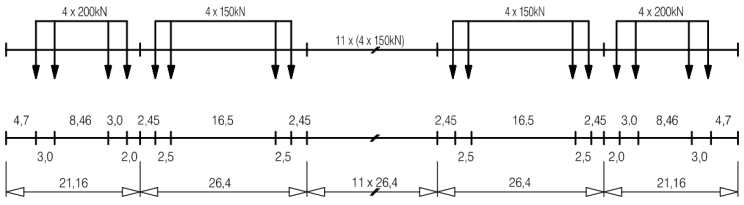

Figure E.3: Train type 3

Type 4 High speed passenger train

$\Sigma Q = 5100\text{kN}$ $V = 250\text{km/h}$ $L = 237{,}60\text{m}$ $q = 21{,}5\text{kN/m'}$

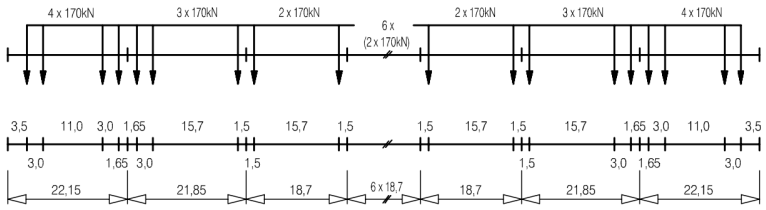

Figure E.4: Train type 4

Type 5 Locomotive-hauled freight train

$\Sigma Q = 21600\text{kN}$ $V = 80\text{km/h}$ $L = 270{,}30\text{m}$ $q = 80{,}0\text{kN/m'}$

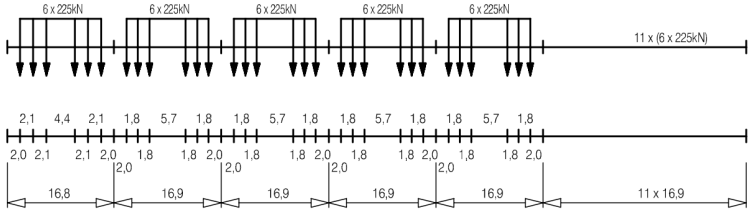

Figure E.5: Train type 5

Type 6 Locomotive-hauled freight train

$\Sigma Q = 14310\text{kN}$ $V = 100\text{km/h}$ $L = 333{,}10\text{m}$ $q = 43{,}0\text{kN/m'}$

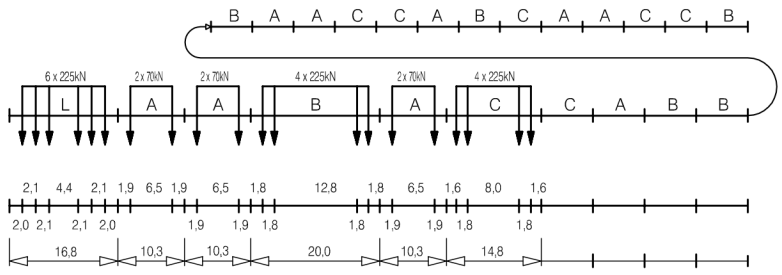

Figure E.6: Train type 6

Type 7 Locomotive-hauled freight train

$\Sigma Q = 10350\text{kN}$ $V = 120\text{km/h}$ $L = 196{,}50\text{m}$ $q = 52{,}7\text{kN/m'}$

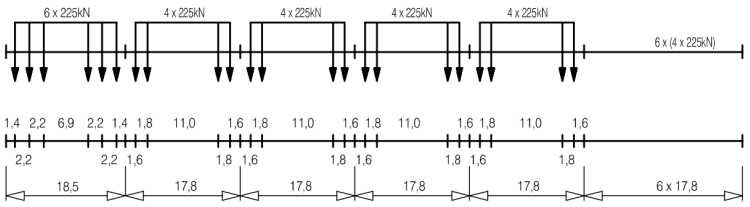

Figure E.7: Train type 7

Type 8 Locomotive-hauled freight train

$\Sigma Q = 10350\text{kN}$ $V = 100\text{km/h}$ $L = 212{,}50\text{m}$ $q = 48{,}7\text{kN/m'}$

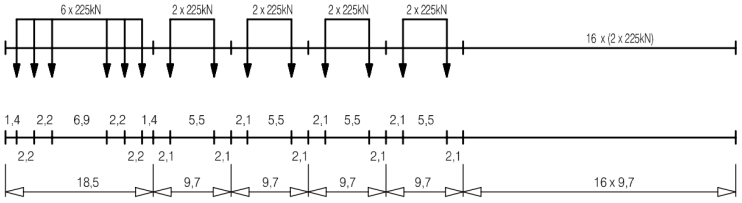

Figure E.8: Train type 8

Type 9 Surburban multiple unit train

$\Sigma Q = 2960\text{kN}$ $V = 120\text{km/h}$ $L = 134{,}80\text{m}$ $q = 22{,}0\text{kN/m'}$

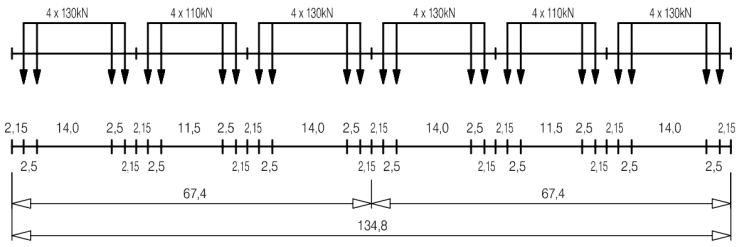

Figure E.9: Train type 9

Type 10 Underground

$\Sigma Q = 3600\text{kN}$ $V = 120\text{km/h}$ $L = 129{,}60\text{m}$ $q = 27{,}8\text{kN/m'}$

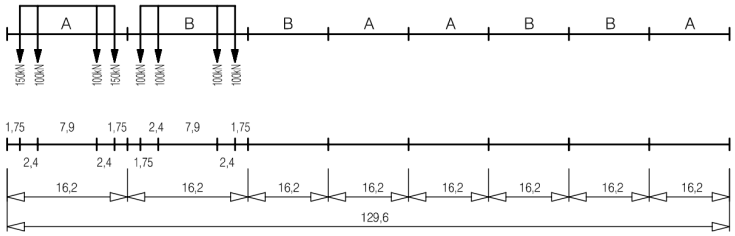

Figure E.10: Train type 10

Type 11 Locomotive-hauled freight train

$\Sigma Q = 11350\text{kN}$ $V = 120\text{km/h}$ $L = 198{,}50\text{m}$ $q = 57{,}2\text{kN/m'}$

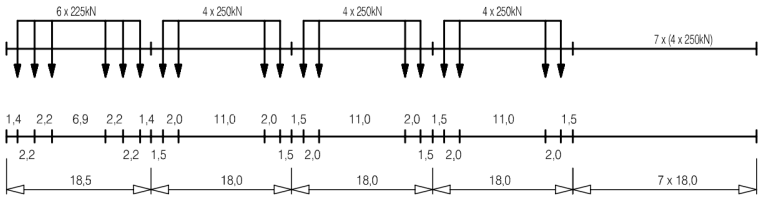

Figure E.11: Train type 11

Type 12 Locomotive-hauled freight train

$\Sigma Q = 11350\text{kN}$ $V = 100\text{km/h}$ $L = 212{,}50\text{m}$ $q = 53{,}4\text{kN/m'}$

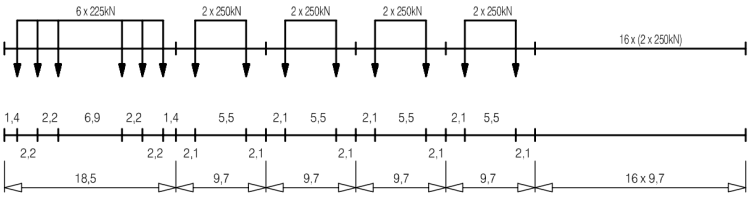

Figure E.12: Train type 12